International Journal of Control
Publication details, including instructions for authors and subscription information:
http://www.informaworld.com/smpp/title~content=t713393989

Limit cycle stability analysis and adaptive control of a multi-compartment model for a pressure-limited respirator and lung mechanics system

VijaySekhar Chellaboina [a]; Wassim M. Haddad [b]; Hancao Li [b];James M. Bailey [c]
[a] Advanced Technology Center, Tata Consultancy Services, Hyderabad, India 500081 [b] School of Aerospace Engineering, Georgia Institute of Technology, Atlanta, GA 30332-0150, USA [c] Department of Anesthesiology, Northeast Georgia Medical Center, Gainesville, GA 30503, USA

Online publication date: 23 April 2010

To cite this Article Chellaboina, VijaySekhar , Haddad, Wassim M. , Li, Hancao andBailey, James M.(2010) 'Limit cycle stability analysis and adaptive control of a multi-compartment model for a pressure-limited respirator and lung mechanics system', International Journal of Control, 83: 5, 940 — 955

To link to this Article: DOI: 10.1080/00207170903502823

URL: http://dx.doi.org/10.1080/00207170903502823

International Journal of Control
Vol. 83, No. 5, May 2010, 940–955

Limit cycle stability analysis and adaptive control of a multi-compartment model for a pressure-limited respirator and lung mechanics system

VijaySekhar Chellaboina[a], Wassim M. Haddad[b]*, Hancao Li[b] and James M. Bailey[c]

[a]*Advanced Technology Center, Tata Consultancy Services, Hyderabad, India 500081;* [b]*School of Aerospace Engineering, Georgia Institute of Technology, Atlanta, GA 30332-0150, USA;* [c]*Department of Anesthesiology, Northeast Georgia Medical Center, Gainesville, GA 30503, USA*

(*Received 28 May 2009; final version received 21 November 2009*)

Acute respiratory failure due to infection, trauma or major surgery is one of the most common problems encountered in intensive care units, and mechanical ventilation is the mainstay of supportive therapy for such patients. In this article, we develop a general mathematical model for the dynamic behaviour of a multi-compartment respiratory system in response to an arbitrary applied inspiratory pressure. Specifically, we use compartmental dynamical system theory and Poincaré maps to model and analyse the dynamics of a pressure-limited respirator and lung mechanics system, and show that the periodic orbit generated by this system is globally asymptotically stable. Furthermore, we show that the individual compartmental volumes, and hence the total lung volume, converge to steady-state end-inspiratory and end-expiratory values. Finally, we develop a model reference direct adaptive controller framework for the multi-compartmental model of a pressure-limited respirator and lung mechanics system where the plant and reference model involve switching and time-varying dynamics. We then apply the proposed adaptive feedback controller framework to stabilise a given limit cycle corresponding to a clinically plausible respiratory pattern.

Keywords: mechanical ventilation; multi-compartment model; bronchial tree; limit cycle analysis; periodic orbits; stability of periodic orbits; Poincaré maps; adaptive control

1. Introduction

Acute respiratory failure due to infection, trauma and major surgery is one of the most common problems encountered in intensive care units and mechanical ventilation is the mainstay of supportive therapy for such patients. Numerous mathematical models of respiratory function have been developed in the hope of better understanding pulmonary function and the process of mechanical ventilation (Campbell and Brown 1963; Wald, Murphy, and Mazzia 1968; Epstein and Epstein 1979; Barbini 1982; Marini and Crooke 1993). However, the models that have been presented in the medical and scientific literature have typically assumed homogenous lung function. For example, in analogy to a simple electrical circuit, the most common model has assumed that the lungs can be viewed as a single compartment characterised by its compliance (the ratio of compartment volume to pressure) and the resistance to air flow into the compartment (Campbell and Brown 1963; Wald *et al.* 1968; Marini and Crooke 1993).

While a few investigators have considered two compartment models, reflecting the fact that there are two lungs (right and left), there has been little interest in more detailed models (Similowski and Bates 1991; Hotchkiss , Crooke, Adams, and Marini 1994; Crooke, Head, and Marini 1996). However, the lungs, especially diseased lungs, are heterogeneous, both functionally and anatomically, and are composed of many subunits, or compartments, that differ in their capacities for gas exchange. Realistic models should take this heterogeneity into account. While more sophisticated models entail greater complexity, since the models are readily presented in the context of dynamical systems theory, sophisticated mathematical tools can be applied to their analysis. Compartmental lung models are described by a state vector, whose components are the volumes of the individual compartments. One interesting and important question is the stability, in the sense of dynamical systems theory, of the model.

For a simple one compartment model, it is easy to demonstrate that the model exhibits an asymptotically stable limit cycle behaviour. And indeed, in clinical practice it appears that the total lung volume converges to the steady-state end-inspiratory and end-expiratory values after the institution of mechanical ventilation. However, a more subtle question for a multi-compartment lung model is whether the volumes in the individual compartments could be unstable, even

*Corresponding author. Email: wm.haddad@aerospace.gatech.edu

ISSN 0020–7179 print/ISSN 1366–5820 online

DOI: 10.1080/00207170903502823
http://www.informaworld.com

when the total volume of the lung (the sum of all the compartment volumes) converges to a steady-state value. That is, is it possible that individual compartment volumes oscillate or even demonstrate chaotic behaviour while the total lung volume is stable?

This question has interesting clinical implications as there is also heterogeneity in the amount of blood flowing to individual subunits of the lung. If there is significant disparity in the ratio of ventilation (reflected in the compartment volume) to blood flow, gas exchange is impaired, resulting in decreases in the oxygen or increases in the carbon dioxide content of blood, which is a serious clinical problem. Instability of the compartment volumes could be reflected in unstable measures of basic pulmonary function, such as oxygen or carbon dioxide levels in the blood. In this article, we first develop a generalised multi-compartment lung model and subsequently analyse its stability properties. Specifically, we use compartmental dynamical system theory and Poincaré maps to model and analyse the dynamics of a pressure-limited respirator and lung mechanics system, and show that the periodic orbit generated by this system is globally asymptotically stable. Furthermore, we show that the individual compartmental volumes, and hence the total lung volume, converge to steady-state end-inspiratory and end-expiratory values.

As noted above, mechanical ventilation of a patient with respiratory failure is one of the most common life-saving procedures performed in the intensive care unit. However, mechanical ventilation is physically uncomfortable due to the noxious interface between the ventilator and patient, and mechanical ventilation evokes substantial anxiety on the part of the patient. This will often be manifested by the patient 'fighting the ventilator'. In this situation, there is dyssynchrony between the ventilatory effort of the patient and the ventilator. The patient will attempt to exhale when the ventilator is trying to expand the lungs or the patient will try to inhale when the ventilator is decreasing airway pressure to allow an exhalation. When patient–ventilator dyssynchrony occurs, at the very least there is excessive work of breathing with subsequent ventilatory muscle fatigue and in the worst case, elevated airway pressures that can actually rupture lung tissue. In this situation, it is a very common clinical practice to sedate patients to minimise 'fighting the ventilator'. Sedative-hypnotic agents act on the central nervous system to ameliorate the anxiety and discomfort associated with mechanical ventilation and facilitate patient–ventilator synchrony.

Using the multi-compartmental model of a pressure-limited respirator and lung mechanics systems developed in the first part of the article, we also develop an adaptive feedback controller for addressing this dyssynchrony for intensive care unit sedation. In particular, we develop a model reference direct adaptive controller framework where the plant and reference model involve switching and time-varying dynamics. Then, we apply the proposed adaptive framework to the multi-compartmental model of a pressure-limited respirator and lung mechanics system. Specifically, we develop an adaptive feedback controller that stabilises a given limit cycle corresponding to a clinically plausible breathing pattern. The proposed adaptive control framework for mechanical ventilation can be used to quantify patient–ventilator dyssynchrony as well as to provide closed-loop control for intensive care unit sedation.

2. Notation and mathematical preliminaries

In this section, we introduce notation, several definitions, and some key results that are necessary for developing the main results of this article. Specifically, for $x \in \mathbb{R}^n$ we write $x \geq\geq 0$ (resp., $x \gg 0$) to indicate that every component of x is nonnegative (resp., positive). In this case, we say that x is *nonnegative* or *positive*, respectively. Likewise, $A \in \mathbb{R}^{n \times m}$ is *nonnegative* or *positive* if every entry of A is nonnegative or positive, respectively, which is written as $A \geq\geq 0$ or $A \gg 0$, respectively. Furthermore, for $A \in \mathbb{R}^{n \times n}$ we write $A \geq 0$ (resp., $A > 0$) to indicate that A is a nonnegative-definite (resp., positive-definite) matrix. In addition, $(\cdot)^{\mathrm{T}}$ denotes transpose, $(\cdot)^{-1}$ denotes inverse and '$\otimes$' denotes the Kronecker product. Let $\overline{\mathbb{R}}_+^n$ and $\mathbb{R}_+^n$ denote the nonnegative and positive orthants of $\mathbb{R}^n$, that is, if $x \in \mathbb{R}^n$, then $x \in \overline{\mathbb{R}}_+^n$ and $x \in \mathbb{R}_+^n$ are equivalent, respectively, to $x \geq\geq 0$ and $x \gg 0$. Finally, let $\mathbf{e}_n \in \mathbb{R}^n$ denote the ones vector of order n, that is, $\mathbf{e}_n = [1, \ldots, 1]^{\mathrm{T}}$; if the order of $\mathbf{e}_n$ is clear from context we simply write $\mathbf{e}$ for $\mathbf{e}_n$.

The following definitions introduce the notions of essentially nonnegative, compartmental and strictly ultrametric matrices.

Definition 2.1 (Haddad, Chellabonia, and Hui 2010)**:** Let $A \in \mathbb{R}^{n \times n}$. A is *essentially nonnegative* if $A_{(i,j)} \geq 0$, $i, j = 1, \ldots, n$, $i \neq j$. A is *compartmental* if A is essentially nonnegative and $A^{\mathrm{T}}\mathbf{e} \leq\leq 0$.

Definition 2.2 (Martinez, Michon, and Martin 1994)**:** Let $A \in \mathbb{R}^{n \times n}$ be such that $A \geq\geq 0$. A is *strictly ultrametric* if A is symmetric, $A_{(i,i)} > \max\{A_{(i,k)} : k = 1, \ldots, n, k \neq i\}$, $i = 1, \ldots, n$, and $A_{(i,j)} \geq \min\{A_{(i,k)}, A_{(k,j)}\}$, $k = 1, \ldots, n$, $i, j = 1, \ldots, n$, $i \neq j$.

The following lemmas and propositions are key in establishing the main results of the article.

Lemma 2.1 (Haddad et al. 2010): *Let $A \in \mathbb{R}^{n\times n}$. Then A is essentially nonnegative if and only if e^{At} is nonnegative for all $t \geq 0$.*

Proposition 2.1: *The following statements hold*:

(i) *Let $\lambda_1, \lambda_2 \geq 0$ be such that $\lambda_1 + \lambda_2 > 0$ and let $A_1, A_2 \in \mathbb{R}^{n\times n}$ be strictly ultrametric. Then $\lambda_1 A_1 + \lambda_2 A_2$ is strictly ultrametric.*

(ii) *Let $x \in \mathbb{R}^n$ be such that $x_i = 0$ or 1, $i = 1, \ldots, n$, and let $P \in \mathbb{R}^{n\times n}$ be a positive diagonal matrix. Then $P + xx^{\mathrm{T}}$ is a strictly ultrametric matrix.*

Proof: Statement (i) is a direct consequence of Definition 2.2. To show (ii) let $A \triangleq P + xx^{\mathrm{T}}$ and note that A is symmetric and

$$A_{(i,j)} = \begin{cases} P_{(i,i)} + x_i^2, & \text{if } i = j, \\ x_i x_j, & \text{if } i \neq j. \end{cases}$$

Hence, if $x_i = 0$, then $\max\{A_{(i,k)} : k = 1, \ldots, n, k \neq i\} = 0$, $i = 1, \ldots, n$, which implies that $A_{(i,i)} = P_{(i,i)} > \max\{A_{(i,k)} : k = 1, \ldots, n, k \neq i\}$, $i = 1, \ldots, n$. Alternatively, if $x_i = 1$, then $A_{(i,i)} = P_{(i,i)} + 1 > \max\{x_k : k = 1, \ldots, n, \quad k \neq i\}$, $i = 1, \ldots, n$. Furthermore, for $i \neq j$, $A_{(i,j)} = x_i x_j$ and

$$\min\{A_{(i,k)}, A_{(k,j)}\} = \begin{cases} 0, & \text{if } x_i x_j = 0, \\ x_k, & \text{otherwise.} \end{cases}$$

In either case, $A_{(i,j)} \geq \min\{A_{(i,k)}, A_{(k,j)}\}$, $k = 1, \ldots, n$, $i, j = 1, \ldots, n$, $i \neq j$, which implies that A is strictly ultrametric. □

Lemma 2.2 (Martinez et al. 1994): *Let $A \in \mathbb{R}^{n\times n}$ be such that $A \geq\geq 0$. If A is strictly ultrametric, then $-A^{-1}$ is essentially nonnegative and $A^{-1}\mathbf{e} \geq\geq 0$.*

Proposition 2.2: *Let $A \in \mathbb{R}^{n\times n}$ and assume that there exists an $n \times n$ matrix $P > 0$ such that*

$$A^{\mathrm{T}} P + PA < 0. \tag{1}$$

Then $e^{A^{\mathrm{T}}} P e^{A} < P$.

Proof: Define $R \triangleq -(A^{\mathrm{T}}P + PA) > 0$ and note that (1) implies

$$P = \int_0^\infty e^{A^{\mathrm{T}}t} R e^{At} \mathrm{d}t. \tag{2}$$

Next, pre- and post-multiplying (2) by $e^{A^{\mathrm{T}}}$ and e^{A}, respectively, yields

$$\begin{aligned} e^{A^{\mathrm{T}}} P e^{A} &= \int_0^\infty e^{A^{\mathrm{T}}(t+1)} R e^{A(t+1)} \mathrm{d}t \\ &= \int_1^\infty e^{A^{\mathrm{T}}t} R e^{At} \mathrm{d}t \\ &= \int_0^\infty e^{A^{\mathrm{T}}t} R e^{At} \mathrm{d}t - \int_0^1 e^{A^{\mathrm{T}}t} R e^{At} \mathrm{d}t \\ &= P - \int_0^1 e^{A^{\mathrm{T}}t} R e^{At} \mathrm{d}t \\ &< P, \end{aligned}$$

which proves the result. □

Remark 2.1: It is well known that A is Hurwitz if and only if e^{A} is Schur. Hence, it follows from Proposition 2.2 that the Lyapunov function candidate $V(x) = x^{\mathrm{T}}Px$ can be used to establish the stability of both A and e^{A}.

In this article, we analyse the stability of periodic orbits using Poincaré maps (Wiggins 2003; Haddad and Chellaboina 2008). To state Poincaré's theorem, consider the nonlinear periodic dynamical system

$$\dot{x}(t) = f(t, x(t)), \quad x(0) = x_0, \quad t \in \mathcal{I}_{x_0}, \tag{3}$$

where $x(t) \in \mathcal{D} \subseteq \mathbb{R}^n$, $t \in \mathcal{I}_{x_0}$, is the system state vector, $\mathcal{D}$ is an open set, $f: [0, \infty) \times \mathcal{D} \to \mathbb{R}^n$ satisfies $f(t, x) = f(t + T, x)$, $x \in \mathcal{D}$, $t \geq 0$, for some $T > 0$, and $\mathcal{I}_{x_0} = [0, \tau_{x_0})$, $0 < \tau_{x_0} \leq \infty$, is the maximal interval of existence for the solution $x(\cdot)$ of (3). A continuously differentiable function $x: \mathcal{I}_{x_0} \to \mathcal{D}$ is said to be a *solution* to (3) on the interval $\mathcal{I}_{x_0} \subseteq [0, \infty)$ with initial condition $x(0) = x_0$ if $x(t)$ satisfies (3) for all $t \in \mathcal{I}_{x_0}$. It is assumed that $f(\cdot, \cdot)$ is such that the solution to (3) is unique for every initial condition in $\mathcal{D}$ and jointly continuous in t and x_0. A sufficient condition ensuring this is Lipschitz continuity of $f(t, \cdot): \mathcal{D} \to \mathbb{R}^n$ for all $t \in [0, t_1]$ and continuity of $f(\cdot, x): [0, t_1] \to \mathbb{R}^n$ for all $x \in \mathcal{D}$. Here, we assume that all solutions to (3) are bounded over $\mathcal{I}_{x_0}$, and hence, by the Peano-Cauchy theorem can be extended to infinity.

Next, we introduce the notions of periodic solutions and periodic orbits for (3). For the next definition, we denote the solution $x(\cdot)$ to (3) with initial conditon $x_0 \in \mathcal{D}$ by $s(t, x_0)$.[1]

Definition 2.3: A solution $s(t, x_0)$ of (3) is *periodic* if there exists a finite time $T > 0$ such that $s(t + T, x_0) = s(t, x_0)$ for all $t \geq 0$. A set $\mathcal{O} \subset \mathcal{D}$ is a *periodic orbit* of (3) if $\mathcal{O} = \{x \in \mathcal{D} : x = s(t, x_0),\ 0 \leq t \leq T\}$ for some periodic solution $s(t, x_0)$ of (3).

Next, we introduce the notions of Lyapunov and asymptotic stability of a periodic orbit of the nonlinear dynamical system (3). For this definition, dist$(p, \mathcal{M})$ denotes the smallest distance from a point p to any point in the set $\mathcal{M}$, that is, $\mathrm{dist}(p, \mathcal{M}) \triangleq \inf_{x\in\mathcal{M}} \|p - x\|$.

Definition 2.4: A periodic orbit $\mathcal{O}$ of (3) is *Lyapunov stable* if, for all $\varepsilon > 0$, there exists $\delta = \delta(\varepsilon) > 0$ such that if $\mathrm{dist}(x_0, \mathcal{O}) < \delta$, then $\mathrm{dist}(s(t, x_0), \mathcal{O}) < \varepsilon$, $t \geq 0$. A periodic orbit $\mathcal{O}$ is *asymptotically stable* if $\mathcal{O}$ is Lyapunov stable and there exists $\varepsilon > 0$ such that if $\mathrm{dist}(x_0, \mathcal{O}) < \varepsilon$, then $\mathrm{dist}(s(t, x_0), \mathcal{O}) \to 0$ as $t \to \infty$.

To proceed, we assume that for the point $p \in \mathcal{D}$, the dynamical system (3) has a periodic solution $s(t, p)$, $t \geq 0$, with period $T > 0$ that generates the periodic orbit $\mathcal{O} \triangleq \{x \in \mathcal{D} : x = s(t, p), 0 \leq t \leq T\}$. Next, let $\mathcal{U} \subset \mathcal{D}$ be a neighbourhood of the point p and define the Poincaré return map $P:\mathcal{U}\to\mathcal{D}$ by

$$P(x)\triangleq s(T,x),\quad x\in\mathcal{U}. \tag{4}$$

Furthermore, define the discrete-time dynamical system given by

$$z(k+1)=P(z(k)),\quad z(0)\in\mathcal{U},\ k\in\overline{\mathbb{Z}}_+, \tag{5}$$

where $\overline{\mathbb{Z}}_+$ denotes the set of nonnegative integers. Clearly $x=p$ is a fixed point of (5) since $p=s(T,p)=P(p)$.

Theorem 2.1: Consider the nonlinear periodic dynamical system (3) with the Poincaré map defined by (4). Assume that the point $p\in\mathcal{D}$ generates the periodic orbit $\mathcal{O}\triangleq\{x\in\mathcal{D}:x=s(t,p),\ 0\le t\le T\}$, where $s(t,p)$, $t\ge 0$, is the periodic solution with period T. Then the following statements hold:

(i) $p\in\mathcal{D}$ is a Lyapunov stable fixed point of (5) if and only if the periodic orbit $\mathcal{O}$ generated by p is Lyapunov stable.
(ii) $p\in\mathcal{D}$ is an asymptotically stable fixed point of (5) if and only if the periodic orbit $\mathcal{O}$ generated by p is asymptotically stable.

Proof: Define $x_1(t)\triangleq x(t)$ and $x_2(t)\triangleq t$, and note that the solution $x(t)$, $t\ge 0$, to the nonlinear periodic dynamical system (3) can be equivalently characterised by the solution $x_1(t)$, $t\ge 0$, to the nonlinear autonomous dynamical system

$$\dot{x}_1(t)=f(x_2(t),x_1(t)),\quad x_1(0)=x_0,\ t\ge 0, \tag{6}$$

$$x_2(t)=t \bmod T,\quad x_2(0)=0. \tag{7}$$

Since $p\in\mathcal{D}$ generates a periodic solution to (3) it follows that the point $[p,0]^{\mathrm{T}}\in\mathcal{D}\times[0,T]$ generates a periodic solution to (6) and (7). Next, it can be shown that the map $P:\mathcal{U}\to\mathcal{D}$ given by (4) is a Poincaré map for (6) and (7) (see Wiggins (2003, p. 127) for details). Now, the result is a direct consequence of the standard Poincaré theorem (Haddad and Chellaboina 2008). □

Finally, in this article, we develop a multi-compartment lung model based on a directed tree architecture. The following definitions are necessary for the main results of this article.

Definition 2.5 (Thulasiraman and Swamy 1992)**:** A *weighted directed graph* $\mathfrak{G}$ is a triple $(\mathcal{V},\mathcal{E},W)$, where $\mathcal{V}=\{v_1,v_2,\ldots,v_N\}$ is the set of *vertices*, $\mathcal{E}=\{e_1,e_2,\ldots,e_M\}\subseteq\mathcal{V}\times\mathcal{V}$ is the set of *edges* and $W\in\mathbb{R}^{N\times N}$ is the weighted *adjacency matrix*. Every edge $e_l\in\mathcal{E}$ corresponds to an ordered pair of vertices $(v_i,v_j)\in\mathcal{V}\times\mathcal{V}$, where v_i and v_j are the *initial* and *terminal vertices* of the edge e_l. In this case, e_l is *incident into* v_j and *incident out of* v_i. The adjacency matrix W is such that $W_{(i,j)}>0$, $i,j=1,\ldots,N$, if $(v_i,v_j)\in\mathcal{E}$, and $W_{(i,j)}=0$, otherwise. The *in-degree* $d_{\mathrm{i}}(v_i)$ of v_i is the number of edges incident into v_i and the *out-degree* $d_{\mathrm{o}}(v_j)$ of v_j is the number of edges incident out of v_j. A *directed path from* v_{i_1} to v_{i_k} is a set of distinct vertices $\{v_{i_1},v_{i_2},\ldots,v_{i_k}\}$ such that $(v_{i_j},v_{i_{j+1}})\in\mathcal{E}$, $j=1,\ldots,k-1$. A vertex v_i is a *root* of $\mathfrak{G}$ if, for every $v_j\neq v_i$, there exist directed paths from v_i to v_j. $\mathfrak{G}$ is *connected* if, for every pair of v_i, $v_j\in\mathcal{V}$, there exists $v_k\in\mathcal{V}$ such that there are directed paths from v_k to v_i and v_k to v_j. A vertex $v_i\in\mathcal{V}$ is a *leaf* of $\mathfrak{G}$ if $d_{\mathrm{o}}(v_i)=0$.

Definition 2.6 (Thulasiraman and Swamy 1992)**:** A weighted directed graph $\mathfrak{G}$ is a *weighted directed tree* if $\mathcal{G}$ is connected and there exists a vertex $v_i\in\mathcal{V}$ such that $d_{\mathrm{i}}(v_i)=0$ and $d_{\mathrm{i}}(v_j)=1$, $v_j\in\mathcal{V}\setminus\{v_i\}$.

Remark 2.2: Note that if $\mathfrak{G}$ is a weighted directed tree, then there exists exactly one root $v_i\in\mathcal{V}$ and exactly one directed path from v_i to v_j for all $v_j\in\mathcal{V}\setminus\{v_i\}$ (see Thulasiraman and Swamy (1992), for details).

3. Compartmental modelling of lung dynamics: dichotomy architecture

In this section, we develop a general mathematical model for the dynamic behaviour of a multi-compartment respiratory system in response to an arbitrary applied inspiratory pressure. Here, we assume that the bronchial tree has a dichotomy architecture (Weibel 1963), that is, in every generation each airway unit branches in two airway units of the subsequent generation. First, however, we start by considering a single-compartment lung model as shown in Figure 1. In this model, the lungs are represented as a single lung unit with compliance c connected to a pressure source by an airway unit with resistance (to air flow) of R. At time $t=0$, an arbitrary pressure $p_{\mathrm{in}}(t)$ is applied to the opening of the parent airway, where $p_{\mathrm{in}}(t)$ is determined by the mechanical ventilator. A typical choice for $p_{\mathrm{in}}(t)$ is $p_{\mathrm{in}}(t)=\alpha t+\beta$,

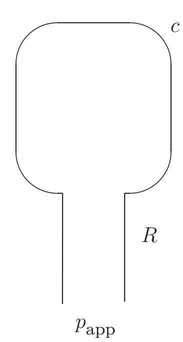

Figure 1. Single-compartment lung model.

where α and β are positive constants. This pressure is applied to the airway opening over the time interval $0 \le t \le T_{\text{in}}$, which is the inspiratory part of the breathing cycle. At time $t = T_{\text{in}}$, the applied airway pressure is released and expiration takes place passively, that is, the external pressure is only the atmospheric pressure $p_{\text{ex}}(t)$ during the time interval $T_{\text{in}} \le t \le T_{\text{in}} + T_{\text{ex}}$, where T_{ex} is the duration of expiration.

The state equation for inspiration (inflation of lung) is given by

$$R_{\text{in}}\dot{x}(t) + \frac{1}{c}x(t) = p_{\text{in}}(t), \quad x(0) = x_0^{\text{in}}, \quad 0 \le t \le T_{\text{in}}, \tag{8}$$

where $x(t) \in \mathbb{R}$, $t \ge 0$, is the lung volume, $R_{\text{in}} \in \mathbb{R}$ is the resistance to air flow during the inspiration period, $x_0^{\text{in}} \in \mathbb{R}_+$ is the lung volume at the start of the inspiration and serves as the system initial condition. Equation (8) is simply a pressure balance equation (Crooke et al. 1996) where the total pressure $p_{\text{in}}(t)$, $t \ge 0$, applied to the compartment is proportional to the volume of the compartment via the compliance and the rate of change of the compartmental volume via the resistance. We assume that expiration is passive (due to elastic stretch of lung unit). During the expiration process, the state equation is given by

$$R_{\text{ex}}\dot{x}(t) + \frac{1}{c}x(t) = p_{\text{ex}}(t), \quad x(T_{\text{in}}) = x_0^{\text{ex}}, \\ T_{\text{in}} \le t \le T_{\text{in}} + T_{\text{ex}}, \tag{9}$$

where $x(t) \in \mathbb{R}$, $t \ge 0$, is the lung volume, $R_{\text{ex}} \in \mathbb{R}$ is the resistance to air flow during the expiration period and $x_0^{\text{ex}} \in \mathbb{R}_+$ is the lung volume at the start of expiration.

Next, we develop the state equations for inspiration and expiration for a 2^n-compartment model, where $n \ge 0$. In this model, the lungs are represented as 2^n lung units which are connected to the pressure source by n generations of airway units, where each airway is divided into two airways of the subsequent generation leading to 2^n compartments (see Figure 2 for a four-compartment model).

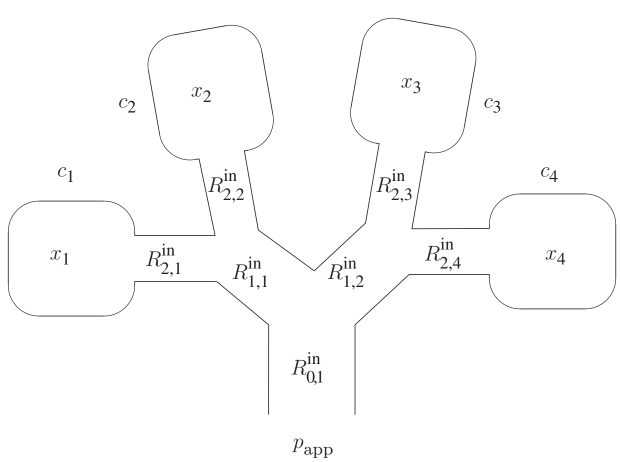

Figure 2. Four-compartment lung model.

Let c_i, $i = 1, 2, \ldots, 2^n$, denote the compliance of each compartment and let $R_{j,i}^{\text{in}}$ (resp., $R_{j,i}^{\text{ex}}$), $i = 1, 2, \ldots, 2^j$, $j = 0, \ldots, n$, denote the resistance (to air flow) of the i-th airway in the j-th generation during the inspiration (resp., expiration) period with R_{01}^{in} (resp., R_{01}^{ex}) denoting the inspiration (resp., expiration) of the *parent* (i.e. 0-th generation) airway. As in the single-compartment model, we assume that a pressure of $p_{\text{in}}(t)$, $t \ge 0$ is applied during inspiration. Next, let x_i, $i = 1, 2, \ldots, 2^n$, denote the lung volume in the i-th compartment so that the state equations for inspiration are given by

$$R_{n,i}^{\text{in}}\dot{x}_i(t) + \frac{1}{c_i}x_i(t) + \sum_{j=0}^{n-1} R_{j,k_j}^{\text{in}} \sum_{l=(k_j-1)2^{n-j}+1}^{k_j 2^{n-j}} \dot{x}_l(t) = p_{\text{in}}(t), \\ x_i(0) = x_{i0}^{\text{in}}, \quad 0 \le t \le T_{\text{in}}, \quad i = 1, 2, \ldots, 2^n, \tag{10}$$

where

$$k_j = \left\lfloor \frac{k_{j+1} - 1}{2} \right\rfloor + 1, \quad j = 0, \ldots, n-1, \quad k_n = i, \tag{11}$$

and $\lfloor q \rfloor$ denotes the *floor function* which gives the largest integer less than or equal to the positive number q.

To further elucidate the inspiration state equation for a 2^n-compartment model, consider the four-compartment model shown in Figure 2 corresponding to a 2-generation lung model. Let x_i, $i = 1, 2, 3, 4$, denote the compartmental volumes. Now, the pressure $\frac{1}{c_i}x_i(t)$ due to the compliance in i-th compartment will be equal to the difference between the external pressure applied and the resistance to air flow at every airway in the path leading from the pressure source to the i-th compartment. In particular, for $i = 3$ (Figure 2),

$$\frac{1}{c_3}x_3(t) = p_{\text{in}}(t) - R_{0,1}^{\text{in}}[\dot{x}_1(t) + \dot{x}_2(t) + \dot{x}_3(t) + \dot{x}_4(t)] \\ - R_{1,2}^{\text{in}}[\dot{x}_3(t) + \dot{x}_4(t)] - R_{2,3}^{\text{in}}\dot{x}_3(t),$$

or, equivalently,

$$R_{2,3}^{\text{in}}\dot{x}_3(t) + R_{1,2}^{\text{in}}[\dot{x}_3(t) + \dot{x}_4(t)] + R_{0,1}^{\text{in}}[\dot{x}_1(t) + \dot{x}_2(t) \\ + \dot{x}_3(t) + \dot{x}_4(t)] + \frac{1}{c_3}x_3(t) = p_{\text{in}}(t).$$

Next, we consider the state equation for the expiration process. As in the single-compartment model we assume that the expiration process is passive and the external pressure applied is $p_{\text{ex}}(t)$, $t \ge 0$. Following an identical procedure as in the inspiration case, we obtain the state equation for expiration as

$$R^{\rm ex}_{n,i}\dot{x}_i(t)+\sum_{j=0}^{n-1}R^{\rm ex}_{j,k_j}\sum_{l=(k_j-1)2^{n-j}+1}^{k_j2^{n-j}}\dot{x}_l(t)+\frac{1}{c_i}x_i(t)=p_{\rm ex}(t),$$
$$x_i(T_{\rm in})=x^{\rm ex}_{i_0},\quad T_{\rm in}\le t\le T_{\rm ex}+T_{\rm in},\quad i=1,2,\ldots,2^n, \tag{12}$$

where k_j is given by (11).

4. State space multi-compartment lung model

In this section, we rewrite the state equations (10) and (12) for inspiration and expiration, respectively, as a switched dynamical system. To describe the dynamics of the multi-compartment lung model in terms of a state space model, define the state vector $x\triangleq[x_1,x_2,\ldots,x_{2^n}]^{\rm T}$, where x_i denotes the lung volume of the i-th compartment. Now, the state equation (10) for inspiration can be rewritten as

$$R_{\rm in}\dot{x}(t)+Cx(t)=p_{\rm in}(t)\mathbf{e},\quad x(0)=x^{\rm in}_0,\quad 0\le t\le T_{\rm in}, \tag{13}$$

where $C\triangleq{\rm diag}[\frac{1}{c_1},\ldots,\frac{1}{c_{2^n}}]$ and

$$R_{\rm in}\triangleq\sum_{j=0}^{n}\sum_{k=1}^{2^j}R^{\rm in}_{j,k}Z_{j,k}Z^{\rm T}_{j,k}, \tag{14}$$

where $Z_{j,k}\in\mathbb{R}^{2^n}$ is such that the l-th element of $Z_{j,k}$ is 1 for all $l=(k-1)2^{n-j}+1,\ (k-1)2^{n-j}+2,\ldots,k2^{n-j}$, $k=1,\ldots,2^j$, $j=0,\ 1,\ldots,n$, and zero elsewhere.

Similarly, the state equation (12) for expiration can be rewritten as

$$R_{\rm ex}\dot{x}(t)+Cx(t)=p_{\rm ex}(t)\mathbf{e},\quad x(T_{\rm in})=x^{\rm ex}_0,$$
$$T_{\rm in}\le t\le T_{\rm ex}+T_{\rm in}, \tag{15}$$

where

$$R_{\rm ex}\triangleq\sum_{j=0}^{n}\sum_{k=1}^{2^j}R^{\rm ex}_{j,k}Z_{j,k}Z^{\rm T}_{j,k}. \tag{16}$$

Note that if $R_{\rm in}$ and $R_{\rm ex}$ are invertible, then (13) and (15) can be equivalently written as

$$\dot{x}(t)=A_{\rm in}x(t)+B_{\rm in}p_{\rm in}(t),\quad x(0)=x^{\rm in}_0,\quad 0\le t\le T_{\rm in}, \tag{17}$$

$$\dot{x}(t)=A_{\rm ex}x(t)+B_{\rm ex}p_{\rm ex}(t),\quad x(T_{\rm in})=x^{\rm ex}_0,$$
$$T_{\rm in}\le t\le T_{\rm ex}+T_{\rm in}, \tag{18}$$

where $A_{\rm in}\triangleq-R_{\rm in}^{-1}C$, $B_{\rm in}\triangleq R_{\rm in}^{-1}\mathbf{e}$, $A_{\rm ex}\triangleq-R_{\rm ex}^{-1}C$ and $B_{\rm ex}\triangleq R_{\rm ex}^{-1}\mathbf{e}$.

The following proposition states and proves several important properties of $R_{\rm in}$, $R_{\rm ex}$, $A_{\rm in}$ and $A_{\rm ex}$ that are essential for the main results of this article.

Proposition 4.1: *Consider the dynamical system* (13) *and* (15). *Then the following statements hold*:

- (i) $R_{\rm in}>0$ *and* $R_{\rm ex}>0$.
- (ii) $A_{\rm in}^{\rm T}C+CA_{\rm in}<0$.
- (iii) $A_{\rm ex}^{\rm T}C+CA_{\rm ex}<0$.
- (iv) $R_{\rm in}$ *and* $R_{\rm ex}$ *are strictly ultrametric.*
- (v) $A_{\rm in}$ *and* $A_{\rm ex}$ *are compartmental and Hurwitz, and* $B_{\rm in}\ge\ge0$ *and* $B_{\rm ex}\ge\ge0$.

Proof: Statement (i) follows from (14) by noting

$$R_{\rm in}\ge\sum_{k=1}^{2^n}R^{\rm in}_{n,k}\ Z_{n,k}\ Z^{\rm T}_{n,k}={\rm diag}[R^{\rm in}_{n,1},\ldots,R^{\rm in}_{n,2^n}]>0,$$

since the l-th element of $Z_{n,k}$ is 1 if $l=k$ and zero otherwise. Similarly, it can be shown that $R_{\rm ex}>0$.

Statements (ii) and (iii) follow immediately by noting that

$$A_{\rm in}^{\rm T}C+CA_{\rm in}=-2CR_{\rm in}^{-1}C<0$$

and

$$A_{\rm ex}^{\rm T}C+CA_{\rm ex}=-2CR_{\rm ex}^{-1}C<0.$$

To show (iv), define

$$R_j^{\rm in}\triangleq\varepsilon R_n^{\rm in}+\sum_{k=1}^{2^j}R^{\rm in}_{j,k}Z_{j,k}Z^{\rm T}_{j,k},\quad j=1,\ldots,n-1,$$

where $R_n^{\rm in}\triangleq{\rm diag}[R^{\rm in}_{n,1},\ldots,R^{\rm in}_{n,2^n}]$ and $\varepsilon=\frac{1}{n-1}$. Note that it follows from Proposition 2.1 that, for every $j\in\{1,\ldots,n\}$, $R_j^{\rm in}$ is strictly ultrametric, and hence, $R_{\rm in}=\sum_{j=1}^{n}R_j^{\rm in}$ is strictly ultrametric. Similarly, it can be shown that $R_{\rm ex}$ is strictly ultrametric.

Finally, to show (v) note that since $R_{\rm in}$ and $R_{\rm ex}$ are strictly ultrametric it follows from Lemma 2.2 that $B_{\rm in}=R_{\rm in}^{-1}\mathbf{e}\ge\ge0$, $B_{\rm ex}=R_{\rm ex}^{-1}\mathbf{e}\ge\ge0$ and $-R_{\rm in}^{-1}$ and $-R_{\rm ex}^{-1}$ are essentially nonnegative. Hence, since C is a positive diagonal matrix, $A_{\rm in}$ and $A_{\rm ex}$ are essentially nonnegative. Now, since $R_{\rm in}^{-1}\mathbf{e}\ge\ge0$ and $R_{\rm ex}^{-1}\mathbf{e}\ge\ge0$ it follows that $A_{\rm in}^{\rm T}\mathbf{e}=-CR_{\rm in}^{-1}\mathbf{e}\le\le0$ and $A_{\rm ex}^{\rm T}\mathbf{e}=-CR_{\rm ex}^{-1}\mathbf{e}\le\le0$, which implies that $A_{\rm in}$ and $A_{\rm ex}$ are compartmental and, by (ii) and (iii), $A_{\rm in}$ and $A_{\rm ex}$ are Hurwitz. □

Remark 4.1: It follows from Proposition 4.1 that $R_{\rm in}$ and $R_{\rm ex}$ are invertible. Hence, $A_{\rm in}$ and $A_{\rm ex}$ are well defined, which implies that the state equations for inspiration and expiration given by (17) and (18), respectively, are well defined.

In this article, we assume that the inspiration process starts from a given initial state $x_0^{\rm in}$ followed by the expiration process where its initial state will be the final state of the inspiration. An inspiration followed by the expiration is called a single *breathing cycle*.

We assume that each breathing cycle is followed by another breathing cycle where the initial condition for the latter breathing cycle is the final state of the former breathing cycle. Furthermore, we assume that the duration of inspiration is $T_{\rm in}$ and that of expiration is $T_{\rm ex}$ so that the total duration of a breathing cycle is $T_{\rm in}+T_{\rm ex}$. It is clear that this process generates a periodic dynamical system with a period $T \triangleq T_{\rm in}+T_{\rm ex}$. Furthermore, the system dynamics switch from inspiration to expiration and back to inspiration. Hence, the dynamics for a breathing cycle can be characterised by the periodic switched dynamical system $\mathcal{G}$ given by

$$\dot{x}(t)=A(t)x(t)+B(t)u(t), \quad x(0)=x_0^{\rm in}, \quad t\geq 0, \tag{19}$$

where

$$A(t)=A(t+T), \quad u(t)=u(t+T), \quad t\geq 0, \tag{20}$$

$$A(t)=\begin{cases} A_{\rm in}, & 0\leq t<T_{\rm in},\\ A_{\rm ex}, & T_{\rm in}\leq t<T,\end{cases} \tag{21}$$

$$B(t)=\begin{cases} B_{\rm in}, & 0\leq t<T_{\rm in},\\ B_{\rm ex}, & T_{\rm in}\leq t<T,\end{cases} \tag{22}$$

$$u(t)=\begin{cases} p_{\rm in}(t), & 0\leq t<T_{\rm in},\\ p_{\rm ex}(t), & T_{\rm in}\leq t<T.\end{cases} \tag{23}$$

The following result shows that the solution to the switched dynamical system (19) is *nonnegative*, that is, for every $x_0^{\rm in}\in\overline{\mathbb{R}}_+^{2^n}$, the solution $x(t)$, $t\geq 0$, to (19) satisfies $x(t)\geq\geq 0$, $t\geq 0$.

Theorem 4.1: *Consider the switched dynamical system* (19) *where* $x_0^{\rm in}\geq\geq 0$. *Then* $x(t)\geq\geq 0$, $t\geq 0$, *where* $x(t)$ *denotes the solution to* (19).

Proof: Note that the solution to (19) over the time interval $[0,T]$ is given by

$$x(t)=\begin{cases} e^{A_{\rm in}t}x_0^{\rm in}+\int_0^t e^{A_{in}(t-\tau)}B_{\rm in}p_{\rm in}(\tau){\rm d}\tau,\\ \qquad 0\leq t\leq T_{\rm in},\\ e^{A_{\rm ex}(t-T_{\rm in})}x_0^{\rm ex}+\int_{T_{\rm in}}^t e^{A_{\rm ex}(t-\tau)}B_{\rm ex}p_{\rm ex}(\tau){\rm d}\tau,\\ \qquad T_{\rm in}\leq t\leq T,\end{cases} \tag{24}$$

where $x_0^{\rm ex}=x(T_{\rm in})$. Now, since $A_{\rm in}$ and $A_{\rm ex}$ are essentially nonnegative (by Proposition 4.1), it follows from Lemma 2.1 that $e^{A_{\rm in}t}\geq\geq 0$ and $e^{A_{\rm ex}t}\geq\geq 0$ for all $t\geq 0$. Hence, $x(t)\geq\geq 0$, $0\leq t\leq T$. Now, the nonnegativity of $x(t)$ for all $t\geq 0$ follows by mathematical induction. □

5. Limit cycle analysis of the multi-compartment lung model

In this section, we characterise and analyse the stability of periodic orbits of the switched dynamical system $\mathcal{G}$ given by (19). First, note that it follows from (24) that

$$x_0^{\rm ex}=x(T_{\rm in})=\Gamma_{\rm in}x_0^{\rm in}+\theta, \tag{25}$$

where

$$\Gamma_{\rm in}\triangleq e^{A_{\rm in}T_{\rm in}}, \tag{26}$$

$$\theta\triangleq e^{A_{\rm in}T_{\rm in}}\int_0^{T_{\rm in}} e^{-A_{\rm in}t}B_{\rm in}p_{\rm in}(t){\rm d}t. \tag{27}$$

Furthermore, note that

$$x(T)=\Gamma_{\rm ex}x_0^{\rm ex}+\delta, \tag{28}$$

where

$$\Gamma_{\rm ex}\triangleq e^{A_{\rm ex}T_{\rm ex}}, \tag{29}$$

$$\delta\triangleq e^{A_{\rm ex}T}\int_{T_{\rm in}}^{T} e^{-A_{\rm ex}t}B_{\rm ex}p_{\rm ex}(t){\rm d}t. \tag{30}$$

Next, let $x_m^{\rm in}$ denote the initial condition for the m-th inspiration (and hence the m-th breathing cycle) and let $x_m^{\rm ex}$ denote the initial condition for the m-th expiration, that is, $x_m^{\rm in}=x(mT)$ and $x_m^{\rm ex}=x(mT+T_{\rm in})$, $m=0,1,\ldots$. Hence, it follows from (25) and (28) that

$$x_1^{\rm in}=\Gamma_{\rm ei}x_0^{\rm in}+\Gamma_{\rm ex}\theta+\delta, \tag{31}$$

where $\Gamma_{\rm ei}\triangleq\Gamma_{\rm ex}\,\Gamma_{\rm in}$. Similarly, it can be shown that

$$x_1^{\rm ex}=\Gamma_{\rm ie}x_0^{\rm ex}+\Gamma_{\rm in}\delta+\theta, \tag{32}$$

where $\Gamma_{\rm ie}\triangleq\Gamma_{\rm in}\Gamma_{\rm ex}$. More generally,

$$x_{m+1}^{\rm in}=\Gamma_{\rm ei}x_m^{\rm in}+\Gamma_{\rm ex}\theta+\delta, \quad m=0,1,\ldots, \tag{33}$$

$$x_{m+1}^{\rm ex}=\Gamma_{\rm ie}x_m^{\rm ex}+\Gamma_{\rm in}\delta+\theta, \quad m=0,1,\ldots. \tag{34}$$

The following proposition states and proves two key properties for $\Gamma_{\rm ei}$ and $\Gamma_{\rm ie}$ which are useful in characterising a periodic orbit for the switched dynamical system $\mathcal{G}$.

Proposition 5.1: *The following statements hold*:

(i) $\Gamma_{\rm ex}^{\rm T}C\Gamma_{\rm ex}<C$ *and* $\Gamma_{\rm in}^{\rm T}C\Gamma_{\rm in}<C$.
(ii) $\Gamma_{\rm ei}^{\rm T}C\Gamma_{\rm ei}<C$ *and* $\Gamma_{\rm ie}^{\rm T}C\Gamma_{\rm ie}<C$.

Proof: It follows from Proposition 4.1 that

$$T_{\rm in}(A_{\rm in}^{\rm T}C+CA_{\rm in})<0,$$

$$T_{\rm ex}(A_{\rm ex}^{\rm T}C+CA_{\rm ex})<0.$$

Hence, it follows from Proposition 2.2 that

$$e^{A_{\rm in}^{\rm T}T_{\rm in}}Ce^{A_{\rm in}T_{\rm in}}<C,$$

$$e^{A_{\rm ex}^{\rm T}T_{\rm ex}}Ce^{A_{\rm ex}T_{\rm ex}}<C,$$

which proves (i).

To prove (ii), pre- and post-multiply the first inequality of (i) by $\Gamma_{\mathrm{in}}^{\mathrm{T}}$ and Γ_{in}, respectively, to obtain

$$\Gamma_{\mathrm{in}}^{\mathrm{T}}\Gamma_{\mathrm{ex}}^{\mathrm{T}}C\Gamma_{\mathrm{ex}}\Gamma_{\mathrm{in}} \le \Gamma_{\mathrm{in}}^{\mathrm{T}}C\Gamma_{\mathrm{in}} < C,$$

where the last inequality follows from (i). This establishes the first inequality of (ii). The second inequality follows in an identical manner. □

For the next result, define $\hat{x}_{\mathrm{in}} \triangleq (I-\Gamma_{\mathrm{ei}})^{-1}(\Gamma_{\mathrm{ex}}\theta+\delta)$ and $\hat{x}_{\mathrm{ex}} \triangleq (I-\Gamma_{\mathrm{ie}})^{-1}(\Gamma_{\mathrm{in}}\delta+\theta)$.

Proposition 5.2: *Consider the switched dynamical system $\mathcal{G}$ given by* (19). *Then, for every $x_0^{\mathrm{in}} \in \overline{\mathbb{R}}_+^{2^n}$, the following statements hold*:

(i) $\lim_{m\to\infty} x_m^{\mathrm{in}} = \hat{x}_{\mathrm{in}}$ *and* $\lim_{m\to\infty} x_m^{\mathrm{ex}} = \hat{x}_{\mathrm{ex}}$.
(ii) *For every* $t \in [0, T_{\mathrm{in}}]$,

$$\lim_{m\to\infty} x(t+mT) = e^{A_{\mathrm{in}}t}\hat{x}_{\mathrm{in}} + \int_0^t e^{A_{\mathrm{in}}(t-\tau)}B_{\mathrm{in}}p_{\mathrm{in}}(\tau)\mathrm{d}\tau,$$

and, for every $t \in [T_{\mathrm{in}}, T]$,

$$\lim_{m\to\infty} x(t+mT+T_{\mathrm{in}}) = e^{A_{\mathrm{ex}}t}\hat{x}_{\mathrm{ex}} + \int_0^t e^{A_{\mathrm{ex}}(t-\tau)}B_{\mathrm{ex}}p_{\mathrm{ex}}(\tau+T_{\mathrm{in}})\mathrm{d}\tau.$$

Proof: It follows from (ii) of Proposition 5.1 that Γ_{ei} and Γ_{ie} are Schur, and hence, $\lim_{m\to\infty}\Gamma_{\mathrm{ei}}^m = 0$ and $\lim_{m\to\infty}\Gamma_{\mathrm{ie}}^m = 0$. Furthermore, $(I-\Gamma_{\mathrm{ei}})^{-1}$ and $(I-\Gamma_{\mathrm{ie}})^{-1}$ exist and are given by

$$(I-\Gamma_{\mathrm{ei}})^{-1} = \sum_{j=0}^{\infty}\Gamma_{\mathrm{ei}}^j, \quad (I-\Gamma_{\mathrm{ie}})^{-1} = \sum_{j=0}^{\infty}\Gamma_{\mathrm{ie}}^j.$$

Next, it follows from (33) and (34) that

$$x_m^{\mathrm{in}} = \Gamma_{\mathrm{ei}}^m x_0^{\mathrm{in}} + \sum_{j=0}^{m-1}\Gamma_{\mathrm{ei}}^j(\Gamma_{\mathrm{ex}}\theta+\delta),$$
$$x_m^{\mathrm{ex}} = \Gamma_{\mathrm{ie}}^m x_0^{\mathrm{ex}} + \sum_{j=0}^{m-1}\Gamma_{\mathrm{ie}}^j(\Gamma_{\mathrm{in}}\delta+\theta),$$

which, by taking limits, yields (i). Now, (ii) follows from (i) and (24). □

Remark 5.1: It follows from Proposition 5.2 that the individual compartmental volumes, and hence the total volume, converge to the steady-state end-inspiratory and end-expiratory values of $(I-\Gamma_{\mathrm{ei}})^{-1}(\Gamma_{\mathrm{ex}}\theta+\delta)$ and $(I-\Gamma_{\mathrm{ie}})^{-1}(\Gamma_{\mathrm{in}}\delta+\theta)$, respectively.

Next, let $\hat{x} \triangleq (I-\Gamma_{\mathrm{ei}})^{-1}(\Gamma_{\mathrm{ex}}\theta+\delta)$ and define the orbit

$$\mathcal{O}_{\hat{x}} \triangleq \{x \in \overline{\mathbb{R}}_+^{2^n} : x = s(t,\hat{x}), \text{ where } s(t,\hat{x}) \text{ is the solution to (19)}\}. \quad (35)$$

With $x_0^{\mathrm{in}} = \hat{x}$ note that $x_m^{\mathrm{in}} = \hat{x}$, $m = 1, 2, \ldots$ or, equivalently, $x(mT) = \hat{x}$, $m = 1, 2, \ldots$ which implies that $\mathcal{O}_{\hat{x}}$ is a periodic orbit of (19). The following theorem presents one of the main results of this article.

Theorem 5.1: *Consider the switched dynamical system $\mathcal{G}$ given by* (19). *Then the periodic orbit $\mathcal{O}_{\hat{x}}$ of $\mathcal{G}$ generated by $x(0) = \hat{x} = (I-\Gamma_{\mathrm{ei}})^{-1}(\Gamma_{\mathrm{ex}}\theta+\delta)$ is globally asymptotically stable.*

Proof: Note that for the periodic orbit $\mathcal{O}_{\hat{x}}$ generated by the point $\hat{x} = (I-\Gamma_{\mathrm{ei}})^{-1}(\Gamma_{\mathrm{ex}}\theta+\delta)$, the Poincaré map is given by

$$z(k+1) = s(T, z(k)) = \Gamma_{\mathrm{ei}}z(k) + \Gamma_{\mathrm{ex}}\theta + \delta, \quad z(0) = x_0^{\mathrm{in}},\ k \in \overline{\mathbb{Z}}_+. \quad (36)$$

Since Γ_{ei} is Schur (by Proposition 5.1) it follows that $\hat{x}$ is an asymptotically stable fixed point of (36). Hence, it follows from Theorem 2.1 that $\mathcal{O}_{\hat{x}}$ is asymptotically stable.

Next, let $\varepsilon > 0$ be such that $\mathrm{dist}(s(t,x_0),\mathcal{O}_{\hat{x}}) \to 0$ for all $x_0 \in \mathcal{D}$ and $\mathrm{dist}\,(x_0,\mathcal{O}_{\hat{x}}) < \varepsilon$. (The existence of such an ε is guaranteed since $\mathcal{O}_{\hat{x}}$ is asymptotically stable.) Now, it follows from (i) of Proposition 5.2 that there exists $m \in \mathbb{Z}_+$ such that $\mathrm{dist}(s(mT,x_0^{\mathrm{in}}),\mathcal{O}_{\hat{x}}) \le \|s(mT,x_0^{\mathrm{in}}) - \hat{x}\| < \varepsilon$. Hence,

$$\lim_{t\to\infty}\mathrm{dist}(s(t,x_0^{\mathrm{in}}),\mathcal{O}_{\hat{x}}) = \lim_{t\to\infty}\mathrm{dist}(s(t-mT, s(mT,x_0^{\mathrm{in}})),\mathcal{O}_{\hat{x}}) = 0,$$

establishing global asymptotic stability of $\mathcal{O}_{\hat{x}}$. □

Remark 5.2: The first part of the proof of Theorem 5.1 shows that the periodic orbit $\mathcal{O}_{\hat{x}}$ is (locally) asymptotically stable. The second part shows that for an arbitrary initial condition $x_0^{\mathrm{in}} \in \overline{\mathbb{R}}_+^{2^n}$, Proposition 5.2 implies that the trajectory of $\mathcal{G}$ comes arbitrarily close to $\mathcal{O}_{\hat{x}}$. Global asymptotic stability now follows from local asymptotic stability. In particular, since $\mathcal{O}_{\hat{x}}$ is asymptotically stable and every trajectory comes arbitrarily close to $\mathcal{O}_{\hat{x}}$, it follows that the trajectory enters the domain of attraction of $\mathcal{O}_{\hat{x}}$, establishing global convergence to $\mathcal{O}_{\hat{x}}$ (and hence, global asymptotic stability).

Remark 5.3: Note that Theorem 5.1 is valid for arbitrary nonnegative functions (possibly discontinuous) $p_{\mathrm{in}}(t)$ and $p_{\mathrm{ex}}(t)$ as long as $\int_0^{T_{\mathrm{in}}} e^{-A_{\mathrm{in}}t}B_{\mathrm{in}}p_{\mathrm{in}}(t)\mathrm{d}t$ and $\int_{T_{\mathrm{in}}}^{T} e^{-A_{\mathrm{ex}}t}B_{\mathrm{ex}}p_{\mathrm{ex}}(t)\mathrm{d}t$ are finite. In the case where $p_{\mathrm{in}}(t) = \alpha t + \beta$ and $p_{\mathrm{ex}}(t) = \gamma$ for some positive constants α, β, and γ, θ and δ are given by

$$\theta = A_{\mathrm{in}}^{-2}[(\alpha I + \beta A_{\mathrm{in}})(e^{A_{\mathrm{in}}T_{\mathrm{in}}} - I) - \alpha A_{\mathrm{in}}T_{\mathrm{in}}]B_{\mathrm{in}},$$
$$\delta = \gamma A_{\mathrm{ex}}^{-1}(e^{A_{\mathrm{ex}}T_{\mathrm{ex}}} - I)B_{\mathrm{ex}}.$$

The following result provides a generalisation to Theorem 5.1.

Theorem 5.2: *Consider the switched dynamical system* $\mathcal{G}$ *given by* (19). *Let* $x(t)$ *and* $y(t)$, $t \geq 0$, *denote the solutions to* (19) *with initial conditions* $x(0) \in \overline{\mathbb{R}}_+^{2^n}$ *and* $y(0) = \hat{x}$. *Then,* $x(t) \to y(t)$ as $t \to \infty$.

Proof: Let $e(t) \triangleq x(t) - y(t)$ so that

$$\dot{e}(t) = A(t)e(t), \quad e(0) = x(0) - \hat{x}, \quad t \geq 0. \tag{37}$$

Now, consider the Lyapunov function candidate $V: \mathbb{R}^{2^n} \to \mathbb{R}$ given by $V(e) = e^{\mathrm{T}}Ce$ so that the Lyapunov derivative of $V(e)$ along the trajectories of (37) is given by

$$\begin{aligned}\dot{V}(e(t)) &= e^{\mathrm{T}}(t)[A^{\mathrm{T}}(t)C + CA(t)]e(t)\\ &\leq \max\{-2e^{\mathrm{T}}(t)CR_{\mathrm{in}}^{-1}Ce(t),\ -2e^{\mathrm{T}}(t)CR_{\mathrm{ex}}^{-1}Ce(t)\}\\ &\leq -2\eta e^{\mathrm{T}}(t)e(t), \quad t \geq 0,\end{aligned}$$

where $\eta \triangleq \min\{\lambda_{\min}(CR_{\mathrm{in}}^{-1}C), \lambda_{\min}(CR_{\mathrm{ex}}^{-1}C)\}$, which implies that $e(t) \to 0$ as $t \to \infty$. □

Remark 5.4: Note that Theorem 5.2 shows that the periodic solution given by $\mathcal{O}_{\hat{x}}$ is globally asymptotically stable (in the sense of stability of motion), and hence, $\mathcal{O}_{\hat{x}}$ is orbitally stable strengthening the conclusion of Theorem 5.1.

Remark 5.5: Note that the error dynamics $e(t)$, $t \geq 0$, given by (37) is a switched dynamical system where each of the switched systems is a linear dynamical system, and $V(e) = e^{\mathrm{T}}Ce$ is a *common* Lyapunov function for both linear systems.

6. A regular dichotomy model

In this section, we present results for a special class of models with a dichotomy architecture. Specifically, we assume that the bronchial tree has a *regular* dichotomy structure (Weibel 1963), that is, for a given branch generation all airflow resistances at the airway units are equal, and hence, for an n-generation model (2^n-compartment model), $R_{j,k}^{\mathrm{in}} = \hat{R}_j^{\mathrm{in}}$ and $R_{j,k}^{\mathrm{ex}} = \hat{R}_j^{\mathrm{ex}}$, $k = 1, 2, \ldots, 2^j$, $j = 0, 1, \ldots, n$, where $\hat{R}_j^{\mathrm{in}} > 0$ and $\hat{R}_j^{\mathrm{ex}} > 0$, $j = 0, \ldots, n$. Furthermore, we assume that $c_k = \hat{c}$, $k = 1, \ldots, 2^n$, that is, the compliance of each compartment is equal. In this case, it can be shown that $C = \frac{1}{\hat{c}} I_{2^n}$ and

$$R_{\mathrm{in}} = \sum_{j=0}^{n} \hat{R}_j^{\mathrm{in}} \big(I_{2^j} \otimes \mathbf{e}_{2^{n-j}} \mathbf{e}_{2^{n-j}}^{\mathrm{T}}\big), \tag{38}$$

$$R_{\mathrm{ex}} = \sum_{j=0}^{n} \hat{R}_j^{\mathrm{ex}} \big(I_{2^j} \otimes \mathbf{e}_{2^{n-j}} \mathbf{e}_{2^{n-j}}^{\mathrm{T}}\big), \tag{39}$$

so that $A_{\mathrm{in}} = -\frac{1}{\hat{c}} R_{\mathrm{in}}^{-1}$, $B_{\mathrm{in}} = R_{\mathrm{in}}^{-1}\mathbf{e}$, $A_{\mathrm{ex}} = -\frac{1}{\hat{c}} R_{\mathrm{ex}}^{-1}$ and $B_{\mathrm{ex}} = R_{\mathrm{ex}}^{-1}\mathbf{e}$. Furthermore, note that $R_{\mathrm{in}}\mathbf{e} = 2^n \hat{R}_{\mathrm{in}}\mathbf{e}$ and $R_{\mathrm{ex}}\mathbf{e} = 2^n \hat{R}_{\mathrm{ex}}\mathbf{e}$, where $\hat{R}_{\mathrm{in}} \triangleq \sum_{j=0}^{n} \frac{\hat{R}_j^{\mathrm{in}}}{2^j}$ and $\hat{R}_{\mathrm{ex}} \triangleq \sum_{j=0}^{n} \frac{\hat{R}_j^{\mathrm{ex}}}{2^j}$, so that $B_{\mathrm{in}} = \frac{1}{2^n \hat{R}_{\mathrm{in}}}\mathbf{e}$, $B_{\mathrm{ex}} = \frac{1}{2^n \hat{R}_{\mathrm{ex}}}\mathbf{e}$ and

$$e^{A_{\mathrm{in}}(T_{\mathrm{in}}-t)} B_{\mathrm{in}} = \frac{1}{2^n \hat{R}_{\mathrm{in}}} e^{-\frac{(T_{\mathrm{in}}-t)}{\hat{c}2^n \hat{R}_{\mathrm{in}}}} \mathbf{e}. \tag{40}$$

Hence,

$$\theta = \frac{e^{-\frac{T_{\mathrm{in}}}{\hat{c}2^n \hat{R}_{\mathrm{in}}}}}{2^n \hat{R}_{\mathrm{in}}} \int_0^{T_{\mathrm{in}}} e^{\frac{t}{\hat{c}2^n \hat{R}_{\mathrm{in}}}} p_{\mathrm{app}}(t)\mathrm{d}t\ \mathbf{e}. \tag{41}$$

Now, using (41) it can be shown that $\hat{x}_{\mathrm{in}}$ is of the form $\gamma\mathbf{e}$, where $\gamma > 0$, and hence, the limit cycle $\mathcal{O}_{\hat{x}} \subset \{\gamma\mathbf{e} : \gamma \geq 0\}$. Thus, it follows that the limiting behaviour of a regular dichotomy lung model exhibits *equipartioning* of the total volume, that is, $x_i(t) \to x_j(t)$ as $t \to \infty$ for all $i, j = 1, 2, \ldots, 2^n$.

Next, we provide a relation between m-generation and n-generation regular dichotomy models, where $m < n$. Let $\hat{R}_{m,j}^{\mathrm{in}}$ and $\hat{R}_{m,j}^{\mathrm{ex}}$ denote the resistances to airflow at a j-th generation airway unit, let $\hat{c}_m$ denote the compliance of each compartment, and let x_i^m denote the i-th compartmental volume in an m-generation model. Here, we assume that

$$x_i^m = \sum_{j=1}^{L} x_{(i-1)L+j}^n, \quad i = 1, \ldots, M, \tag{42}$$

where $L \triangleq 2^{n-m}$ and $M \triangleq 2^m$, that is, each compartment of m-generation model is equivalent to L compartments of the n-generation model so that the total volumes in both models are equal. Note that (42) may be written as

$$x^m = (I_M \otimes \mathbf{e}_L^{\mathrm{T}}) x^n, \tag{43}$$

where $x^m = [x_1^m, \ldots, x_M^m]$ and $x^n = [x_1^n, \ldots, x_N^n]$, and where $N \triangleq 2^n$.

Now, consider the n-generation state equation for inspiration given by

$$R_{\mathrm{in}}^n \dot{x}^n(t) + \frac{1}{\hat{c}_n} x^n(t) = p_{\mathrm{in}}(t)\mathbf{e}_N, \quad x^n(0) = x_{\mathrm{in},0}^n, \quad 0 \leq t \leq T_{\mathrm{in}}, \tag{44}$$

where

$$R_{\mathrm{in}}^n = \sum_{j=0}^{n} \hat{R}_{n,j}^{\mathrm{in}} (I_{2^j} \otimes \mathbf{e}_{2^{n-j}} \mathbf{e}_{2^{n-j}}^{\mathrm{T}}). \tag{45}$$

In this case, it can be shown that

$$(I_M \otimes \mathbf{e}_L^{\mathrm{T}})(I_{2^j} \otimes \mathbf{e}_{2^{n-j}} \mathbf{e}_{2^{n-j}}^{\mathrm{T}}) = \begin{cases} 2^L (I_{2^j} \otimes \mathbf{e}_{2^{m-j}} \mathbf{e}_{2^{m-j}}^{\mathrm{T}}), & j < m, \\ 2^{n-j} (I_M \otimes \mathbf{e}_L^{\mathrm{T}}), & j \geq m. \end{cases} \tag{46}$$

Now, pre-multiplying (45) by $(I_M \otimes \mathbf{e}_L^{\mathrm{T}})$ and using (43) and (46) yields

$$\sum_{j=0}^{m-1} 2^L \hat{R}_{n,j}^{\mathrm{in}} (I_{2^j} \otimes \mathbf{e}_{2^{n-j}} \mathbf{e}_{2^{n-j}}^{\mathrm{T}}) \dot{x}^n(t) + \sum_{j=m}^{n} 2^{n-j} \hat{R}_{n,j}^{\mathrm{in}} \dot{x}^m(t) + \frac{1}{\hat{c}^n} x^m(t) = 2^L p_{\mathrm{in}}(t) \mathbf{e}_M. \quad (47)$$

Next, note that $(I_{2^j} \otimes \mathbf{e}_{2^{m-j}} \mathbf{e}_{2^{n-j}}^{\mathrm{T}}) \dot{x}^n(t) = (I_{2^j} \otimes \mathbf{e}_{2^{m-j}} \mathbf{e}_{2^{m-j}}^{\mathrm{T}}) \dot{x}^m(t)$ so that (47) can be written as

$$\sum_{j=0}^{m-1} \hat{R}_{n,j}^{\mathrm{in}} (I_{2^j} \otimes \mathbf{e}_{2^{m-j}} \mathbf{e}_{2^{m-j}}^{\mathrm{T}}) \dot{x}^m(t) + \sum_{j=m}^{n} 2^{m-j} \hat{R}_{n,j}^{\mathrm{in}} \dot{x}^m(t) + \frac{1}{2^L \hat{c}^n} x^m(t) = p_{\mathrm{in}}(t) \mathbf{e}_M. \quad (48)$$

Comparing (48) with the m-generation model given by

$$R_{\mathrm{in}}^m \dot{x}^m(t) + \frac{1}{\hat{c}_m} x^m(t) = p_{\mathrm{in}}(t) \mathbf{e}_M, \quad (49)$$

yields $\hat{c}_m = 2^{n-m} \hat{c}_n$ and

$$R_{\mathrm{in}}^m = \sum_{j=0}^{m-1} \hat{R}_{n,j}^{\mathrm{in}} (I_{2^j} \otimes \mathbf{e}_{2^{m-j}} \mathbf{e}_{2^{m-j}}^{\mathrm{T}}) + \sum_{j=m}^{n} 2^{m-j} \hat{R}_{n,j}^{\mathrm{in}} I_M,$$

or, equivalently,

$$\hat{R}_{m,j}^{\mathrm{in}} = \hat{R}_{n,j}^{\mathrm{in}}, \quad j = 0, 1, \ldots, m-1, \quad (50)$$

$$\hat{R}_{m,m}^{\mathrm{in}} = \sum_{j=m}^{n} \frac{\hat{R}_{n,j}^{\mathrm{in}}}{2^{j-m}}. \quad (51)$$

Similarly, it can be shown that

$$\hat{R}_{m,j}^{\mathrm{ex}} = \hat{R}_{n,j}^{\mathrm{ex}}, \quad j = 0, 1, \ldots, m-1, \quad (52)$$

$$\hat{R}_{m,m}^{\mathrm{ex}} = \sum_{j=m}^{n} \frac{\hat{R}_{n,j}^{\mathrm{ex}}}{2^{j-m}}. \quad (53)$$

7. A general tree structure model

In this section, we extend the model presented in Sections 3–5 to the case where the bronchial tree has a general tree architecture (Horsfield and Cumming 1975; Horsfield 1990; Kitaoka and Suki 1997). The general tree structure includes the regular and irregular dichotomy (Weibel 1963). Specifically, let the bronchial tree be represented by a weighted directed tree $\mathfrak{G} = (\mathcal{V}, \mathcal{E}, R)$, where each vertex corresponds to a branching point of an airway unit or the terminal compartment (alveolus) of the lung. In this case, the trachea corresponds to the root v_1 of the tree and all the alveoli correspond to the leaves of the tree. Every edge, $(v_l, v_m) \in \mathcal{E}$ corresponds to an airway unit and $R_{(l,m)}$, the weight of the edge, corresponds to the resistance of the airway unit; we use $R_{(l,m)} = R_{l,m}^{\mathrm{in}}$ and $R_{(l,m)} = R_{l,m}^{\mathrm{ex}}$ for resistance during inspiration and expiration, respectively.

Let $\mathcal{L} \triangleq \{v_i \in \mathcal{V} : v_i \text{ is a leaf of } \mathfrak{G}\}$ and let the number of leaves of $\mathfrak{G}$ (or, equivalently, compartments of the lung) be n so that $\mathcal{L} = \{v_{i_1}, v_{i_2}, \ldots, v_{i_n}\}$, where $i_k \in \{1, 2, \ldots, N\}$, $k = 1, 2, \ldots, n$, and N is the number of vertices of the graph. To develop the dynamical model for the inspiration process, let c_k, $k = 1, 2, \ldots, n$, denote the compliance of each compartment, and let x_k, $k = 1, 2, \ldots, n$, denote the lung volume in the k-th compartment so that the state equations for inspiration are given by

$$\frac{1}{c_k} x_k(t) + \sum_{(v_l, v_m) \in \mathcal{P}_k} R_{l,m}^{\mathrm{in}} \sum_{v_{i_j} \in \mathcal{L}_{l,m}} \dot{x}_j(t) = p_{\mathrm{in}}(t),$$

$$x_i(0) = x_{k0}^{\mathrm{in}}, \quad 0 \le t \le T_{\mathrm{in}}, \quad k = 1, 2, \ldots, n, \quad (54)$$

where

$$\mathcal{P}_k \triangleq \{(v_l, v_m) \in \mathcal{E} : (v_l, v_m) \text{ belongs to the directed path from the root of } \mathfrak{G} \text{ to } v_{i_k}\} \quad (55)$$

and, for each $l, m \in \{1, \ldots, N\}$ such that $(v_l, v_m) \in \mathcal{E}$,

$$\mathcal{L}_{l,m} \triangleq \{v_{i_k} \in \mathcal{L} : \text{ there exists a directed path from } v_m \text{ to } v_{i_k}, \ k = 1, \ldots, n\}. \quad (56)$$

Next, let $x \triangleq [x_1, \ldots, x_{2^n}]^{\mathrm{T}}$ so that (54) can be written as

$$R_{\mathrm{in}} \dot{x}(t) + C x(t) = p_{\mathrm{in}}(t) \mathbf{e}, \quad x(0) = x_0^{\mathrm{in}}, \quad 0 \le t \le T_{\mathrm{in}},$$

where $C \triangleq \mathrm{diag}[\frac{1}{c_1}, \ldots, \frac{1}{c_{2^n}}]$ and

$$R_{\mathrm{in}} = \sum_{(v_l, v_m) \in \mathcal{E}} R_{l,m}^{\mathrm{in}} Z_{l,m} Z_{l,m}^{\mathrm{T}}, \quad (57)$$

where $Z_{l,m} \in \mathbb{R}^n$ is such that the k-th element of $Z_{l,m}$ is 1 if $v_{i_k} \in \mathcal{L}_{l,m}$ and 0 otherwise.

An identical procedure yields the state equations for expiration given by

$$R_{\mathrm{ex}} \dot{x}(t) + C x(t) = p_{\mathrm{ex}}(t) \mathbf{e}, \quad x(T_{\mathrm{in}}) = x_0^{\mathrm{ex}}, \ T_{\mathrm{in}} \le t \le T, \quad (58)$$

where

$$R_{\mathrm{ex}} = \sum_{(v_l, v_m) \in \mathcal{E}} R_{l,m}^{\mathrm{ex}} Z_{l,m} Z_{l,m}^{\mathrm{T}}. \quad (59)$$

Note that it can be easily shown that $R_{\mathrm{in}} > 0$ and $R_{\mathrm{ex}} > 0$, and it follows from (57), (59) and Proposition 2.1 that R_{in} and R_{ex} are strictly ultrametric. Hence, for a general tree structure model all of the results of Sections 4 and 5 are valid with $R_{\rm in}$ and $R_{\rm ex}$ given by (57) and (59), respectively.

To illustrate the general tree structure lung model, consider the five-compartment model shown in Figure 3. Here, the bronchial tree is represented by a weighted directed tree $\mathfrak{G} = (\mathcal{V}, \mathcal{E}, R)$ consisting of nine nodes $\mathcal{V} = \{v_1, v_2, \ldots, v_9\}$ and eight edges $\mathcal{E} = \{(v_1, v_2), (v_2, v_3), (v_2, v_4), (v_3, v_5), (v_3, v_6), (v_3, v_7), (v_4, v_8), (v_4, v_9)\}$. In this case, the set of leaves $\mathcal{L} = \{v_5, v_6, \ldots, v_9\}$ corresponds to the five compartments of the lung. Let $v_{i_k} = v_{k+4}$, $k = 1, \ldots, 5$. Now, the pressure $\frac{1}{c_k} x_k(t)$ due to the compliance in k-th compartment will be equal to the difference between the external pressure applied and the resistance to air flow at every airway in the path leading from the pressure source (the root v_1) to the k-th compartment. In particular, for $k = 3$ (Figure 3),

$$\frac{1}{c_3} x_3(t) = p_{\rm in}(t) - R^{\rm in}_{1,2}[\dot{x}_1(t) + \dot{x}_2(t) + \dot{x}_3(t) + \dot{x}_4(t) + \dot{x}_5(t)] - R^{\rm in}_{2,3}[\dot{x}_1(t) + \dot{x}_2(t) + \dot{x}_3(t)] - R^{\rm in}_{3,7}\dot{x}_3(t),$$

or, equivalently,

$$\frac{1}{c_3} x_3(t) + \sum_{(v_l, v_m) \in \mathcal{P}_3} R^{\rm in}_{l,m} \sum_{v_{i_j} \in \mathcal{L}_{l,m}} \dot{x}_j(t) = p_{\rm in}(t), \tag{60}$$

where

$$\mathcal{P}_3 = \{(v_1, v_2), (v_2, v_3), (v_3, v_7)\},$$
$$\mathcal{L}_{1,2} = \{v_5, v_6, v_7, v_8, v_9\},$$
$$\mathcal{L}_{2,3} = \{v_5, v_6, v_7\},$$
$$\mathcal{L}_{3,7} = \{v_7\}.$$

8. Direct adaptive control for switched systems

In this section, we consider the problem of adaptive tracking of uncertain switching systems. Specifically, consider the controlled uncertain switched system $\mathcal{G}$ with time-varying dynamics given by

$$\dot{x}_{\rm p}(t) = A_{\rm p}(t) x_{\rm p}(t) + B_{\rm p}(t) u(t), \quad x_{\rm p}(0) = x_{\rm p0}, \ t \geq 0, \tag{61}$$

where $x_{\rm p}(t) \in \mathbb{R}^n$, $t \geq 0$, is the state vector, $u(t) \in \mathbb{R}^p$, $t \geq 0$, is the control input, and $A_{\rm p}(t) \in \mathbb{R}^{n \times n}$, $t \geq 0$, and $B_{\rm p}(t) \in \mathbb{R}^{n \times p}$, $t \geq 0$, are *unknown* time-varying matrices. The control input $u(\cdot)$ in (61) is restricted to the class of *admissible controls* consisting of measurable functions such that $u(t) \in \mathbb{R}^p$, $t \geq 0$. Furthermore, for the uncertain switched system $\mathcal{G}$, we assume that $A_{\rm p}(\cdot)$ and $B_{\rm p}(\cdot)$ are piecewise continuous functions and we assume that the required properties for the existence and uniqueness of solutions are satisfied; that is, $A_{\rm p}(\cdot)$, $B_{\rm p}(\cdot)$, and $u(\cdot)$ satisfy sufficient regularity conditions such that (61) has a unique solution forward in time.

Next, consider a reference model given by

$$\dot{x}_{\rm m}(t) = A_{\rm m}(t) x_{\rm m}(t) + B_{\rm m}(t) r(t), \quad x_{\rm m}(0) = x_{\rm m0}, \ t \geq 0, \tag{62}$$

where $x_{\rm m}(t) \in \mathbb{R}^n$, $t \geq 0$, is the state vector, $r(t) \in \mathbb{R}^p$, $t \geq 0$, is the reference input, and $A_{\rm m}(t) \in \mathbb{R}^{n \times n}$, $t \geq 0$, and $B_{\rm m}(t) \in \mathbb{R}^{n \times p}$, $t \geq 0$, are known matrices. Moreover, let $A_{\rm m}(t)$, $t \geq 0$, satisfy

$$A^{\rm T}_{\rm m}(t) C_{\rm m} + C_{\rm m} A_{\rm m}(t) \leq -\varepsilon_{\rm m} I, \quad t \geq 0, \tag{63}$$

where $\varepsilon_{\rm m} > 0$ and $C_{\rm m} \in \mathbb{R}^{n \times n}$ is positive definite. Furthermore, we assume that $A_{\rm m}(\cdot)$ and $B_{\rm m}(\cdot)$ are piecewise continuous and are such that (63) has a unique solution for all $t \geq 0$ and $x_{\rm m}(t)$ is uniformly bounded for all $x_{\rm m0} \in \mathbb{R}^n$ and $t \geq 0$.

For the next result, we assume that there exist a positive-definite matrix $Q^* \in \mathbb{R}^{p \times p}$ and a matrix $\Theta^* \in \mathbb{R}^{p \times n}$ such that the compatibility conditions

$$B_{\rm p}(t) Q^* = B_{\rm m}(t), \quad t \geq 0, \tag{64}$$

$$A_{\rm p}(t) + B_{\rm p}(t) \Theta^* = A_{\rm m}(t), \quad t \geq 0, \tag{65}$$

are satisfied.

Theorem 8.1: *Consider the uncertain system* $\mathcal{G}$ *with linear time-varying dynamics given by* (61) *and the reference model given by* (62), *and assume the compatibility conditions* (64) *and* (65) *hold. Then the adaptive feedback control law*

$$u(t) = \Theta(t) x_{\rm p}(t) + Q(t) r(t), \tag{66}$$

where $\Theta(t) \in \mathbb{R}^{p \times n}$, $t \geq 0$, *and* $Q(t) \in \mathbb{R}^{p \times p}$, $t \geq 0$, *with updated laws*

$$\dot{\Theta}(t) = -B^{\rm T}_{\rm m}(t) C_{\rm m} e(t) x^{\rm T}_{\rm p}(t) \Gamma_{\Theta}, \quad \Theta(0) = \Theta_0, \ t \geq 0, \tag{67}$$

$$\dot{Q}(t) = -B^{\rm T}_{\rm m}(t) C_{\rm m} e(t) r^{\rm T}(t) \Gamma_Q, \ Q(0) = Q_0, \tag{68}$$

where $\Gamma_{\Theta} \in \mathbb{R}^{n \times n}$ *and* $\Gamma_Q \in \mathbb{R}^{p \times p}$ *are positive definite and* $e(t) \triangleq x_{\rm p}(t) - x_m(t)$, *guarantees that the solution*

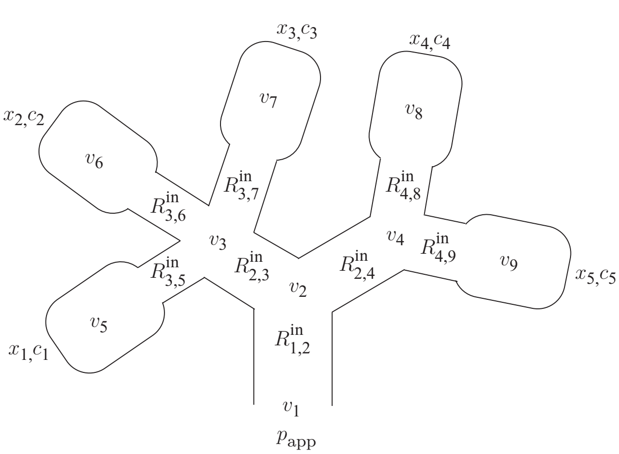

Figure 3. Five-compartment tree structure model.

$(x_p(t), \Theta(t), Q(t))$ *of the closed-loop system given by* (61), (62), (66), (67) *and* (68) *is uniformly bounded for all* $(x_{p0}, \Theta_0, Q_0) \in \mathbb{R}^n \times \mathbb{R}^{p\times n} \times \mathbb{R}^{p\times p}$ *and* $t \geq 0$, *and* $x_p(t) \to x_m(t)$ *as* $t \to \infty$.

Proof: Note that with $u(t)$, $t \geq 0$, given by (66) it follows from (61) that

$$\dot{x}_p(t) = A_p(t)x_p(t) + B_p(t)\Theta(t)x_p(t) + B_p(t)Q(t)r(t), \quad x_p(0) = x_{p0}, \ t \geq 0, \tag{69}$$

or, equivalently, using (64) and (65),

$$\begin{aligned}\dot{x}_p(t) &= A_p(t)x_p(t) + B_p(t)[\Theta^* + \Theta(t) - \Theta^*]x_p(t) \\ &\quad + B_p(t)[Q^* + Q(t) - Q^*]r(t) \\ &= [A_p(t) + B_p(t)\Theta^*]x_p(t) + B_p(t)[\Theta(t) - \Theta^*]x_p(t) \\ &\quad + B_p(t)Q^*r(t) + B_p(t)[Q(t) - Q^*]r(t) \\ &= A_m(t)x_p(t) + B_m(t)r(t) + B_p(t)[\Theta(t) - \Theta^*]x_p(t) \\ &\quad + B_p(t)[Q(t) - Q^*]r(t) \\ &= A_m(t)x_p(t) + B_m(t)r(t) + B_p(t)\Phi^T(t)x_p(t) \\ &\quad + B_p(t)\Psi^T(t)r(t), \quad x_p(0) = x_0, \ t \geq 0,\end{aligned} \tag{70}$$

where $\Phi^T(t) \triangleq \Theta(t) - \Theta^*$ and $\Psi^T(t) \triangleq Q(t) - Q^*$. Now, it follows from (62) and (70) that

$$\dot{e}(t) = A_m(t)e(t) + B_p(t)\Phi^T(t)x_p(t) + B_p(t)\Psi^T(t)r(t), \quad e(0) = x_{p0} - x_{m0}, \ t \geq 0. \tag{71}$$

To show uniform boundedness of the closed-loop system (67), (68) and (71) consider the continuously differentiable function

$$V(e, \Phi, \Psi) = e^T C_m e + \mathrm{tr}\Gamma_Q^{-1}\Psi Q^{*-1}\Psi^T + \mathrm{tr}\Gamma_\Theta^{-1}\Phi Q^{*-1}\Phi^T, \tag{72}$$

and note that $V(0,0,0) = 0$. Since C_m, Γ_Q, Γ_Θ, and Q^* are positive definite, $V(e, \Psi, \Phi) > 0$ for all $(e, \Phi, \Psi) \neq (0,0,0)$. In addition, $V(e, \Phi, \Psi)$ is radially unbounded. Now, using (67) and (68), it follows that the derivative of $V(\cdot,\cdot,\cdot)$ along the closed-loop system trajectories is given by

$$\begin{aligned}\dot{V}&(e(t), \Phi(t), \Psi(t)) \\ &= e^T(t)\big[A_m^T(t)C_m + C_m A_m(t)\big]e(t) \\ &\quad + 2e^T(t)C_m B_p(t)\Phi^T(t)x_p(t) \\ &\quad + 2e^T(t)C_m B_p(t)\Psi^T(t)r(t) + 2\mathrm{tr}\ \Gamma_\Theta^{-1}\Phi(t)Q^{*-1}\dot{\Phi}^T(t) \\ &\quad + 2\mathrm{tr}\ \Gamma_Q^{-1}\Psi(t)Q^{*-1}\dot{\Psi}^T(t) \\ &= e^T(t)\big[A_m^T(t)C_m + C_m A_m(t)\big]e(t) \\ &\quad + 2e^T(t)C_m B_p(t)\Phi^T(t)x_p(t) \\ &\quad + 2e^T(t)C_m B_p(t)\Psi^T(t)r(t) \\ &\quad - 2\mathrm{tr}\Psi(t)Q^{*-1}B_m^T(t)C_m e(t)r^T(t) \\ &\quad - 2\mathrm{tr}\ \Phi(t)Q^{*-1}B_m^T(t)C_m e(t)x_p^T(t) \\ &= e^T(t)\big[A_m^T(t)C_m + C_m A_m(t)\big]e(t) \\ &\leq -\varepsilon_m e^T(t)e(t), \ t \geq 0.\end{aligned} \tag{73}$$

Hence, it follows from Corollary 2.4 of Haddad, Chellabonia, and Nersesov (2006, p. 68) that $(e(t), \Phi(t), \Psi(t))$ is uniformly bounded for all $t \geq 0$, and hence, $(x_p(t), \Theta(t), Q(t))$ is uniformly bounded for all $(x_{p0}, \Theta_0, Q_0) \in \mathbb{R}^n \times \mathbb{R}^{p\times n} \times \mathbb{R}^{p\times p}$ and $t \geq 0$.

Finally, with $W_1(e, \Phi, \Psi) = W_2(e, \Phi, \Psi) = V(e, \Phi, \Psi)$ and $W(e, \Phi, \Psi) = \varepsilon_m e^T e$, it follows from Theorem 2.5 of Haddad et al. (2006) that $(e(t), \Phi(t), \Psi(t)) \to \mathcal{R}$ as $t \to \infty$, where $\mathcal{R} \triangleq \{(e, \Phi, \Psi) : W(e, \Phi, \Psi) = 0\} = \{(e, \Phi, \Psi) : e = 0\}$. In particular, note that

$$\begin{aligned}\dot{W}&(e(t), \Phi(t), \Psi(t)) \\ &= 2\varepsilon_m e^T \dot{e} = 2\varepsilon_m e^T(t)\big[A_m(t)e(t) + B_p(t)\Phi^T(t)x_p(t) \\ &\quad + B_p(t)\Psi^T(t)r(t)\big]\end{aligned} \tag{74}$$

is bounded for all $t \geq 0$, and hence, all conditions of Theorem 2.5 of Haddad et al. (2006, p. 54) are satisfied proving that $e(t) \to 0$ as $t \to \infty$ or, equivalently, $x_p(t) \to x_m(t)$ as $t \to \infty$. □

Remark 8.1: Although the form of the adaptive control law given in Theorem 8.1 is identical to that of the standard model reference adaptive controllers provided in the literature (see e.g. Narendra and Annaswamy 1989), the dynamics of the system considered in Theorem 8.1 is not Lipschitz continuous, and hence, standard proofs involving Barbalat's lemma do not hold. Consequently, Theorem 8.1 requires the more general result given by Theorem 2.5 of Haddad et al. (2006).

Remark 8.2: It is important to note that the adaptive laws (67) and (68) do *not* require explicit knowledge of Q^* or Θ^*. Furthermore, no specific structure on the uncertain dynamics $A_p(\cdot)$ and $B_p(\cdot)$ is required as long as the compatibility conditions (64) and (65) are satisfied.

9. Direct adaptive control for the compartment lung model

In this section, we demonstrate the utility of the proposed direct adaptive control framework for the multi-compartmental lung model developed in Section 4. First, we choose the reference model (62) to correspond to a respiratory system producing a plausible breathing pattern. Specifically, let $A_m(t) = -R_m^{-1}(t)C_m$ and $B_m(t) = R_m^{-1}(t)\mathbf{e}$, where

$$R_m(t) = \begin{cases} R_{in\_m}, & 0 \leq t < T_{in}, \\ R_{ex\_m}, & T_{in} \leq t < T, \end{cases} \tag{75}$$

and where $R_m(t) = R_m(t+T)$, $t > T$. Here, R_{in_m}, R_{ex_m}, C_m and $r(t)$, $t \geq 0$, are chosen appropriately to obtain the desirable breathing pattern. It follows from Theorem 5.1 that $x_m(t)$, $t \geq 0$, converges to a stable limit cycle, and hence, $x_m(t)$, $t \geq 0$, is uniformly bounded.

Next, we assume that the switched system (61) is such that $A_p(t) = -R_p^{-1}(t)C_p$ and $B_p(t) = R_p^{-1}(t)\mathbf{e}$, where

$$R_p(t) = \begin{cases} R_{in\_p}, & 0 \leq t < T_{in}, \\ R_{ex\_p}, & T_{in} \leq t < T, \end{cases} \quad (76)$$

and where $R_p(t) = R_p(t+T)$, $t > T$, so that (61) has the form of a lung mechanics model. Here, we assume that R_{in_p}, R_{ex_p} and C_p are *unknown* and we use Theorem 8.1 to design an adaptive controller $u(t)$, $t \geq 0$, such that $x_p(t) \to x_m(t)$ as $t \to \infty$.

In order to apply Theorem 8.1, we need to show that the compatibility conditions (64) and (65) hold. The following proposition provides sufficient conditions under which (64) and (65) hold for the compartmental lung model. Note that in this case $p = 1$.

Proposition 9.1: *Let* $W \triangleq R_{in\_p}R_{in\_m}^{-1}$. *Assume that the following conditions hold*:

(i) $R_{in\_p}R_{in\_m}^{-1} = R_{ex\_p}R_{ex\_m}^{-1}$.
(ii) *There exists a positive scalar* Q^* *such that* $W\mathbf{e} = Q^*\mathbf{e}$.
(iii) *There exists* $\Theta^* \in \mathbb{R}^{1\times n}$ *such that* $C_p = WC_m + \mathbf{e}\Theta^*$.

Then (64) *and* (65) *hold.*

Proof: The proof follows by noting that (i) and (ii) imply (64) holds, while (i) and (iii) imply (65) holds. □

Remark 9.1: In the absence of switching, conditions (ii) and (iii) are standard for model reference adaptive control (Narendra and Annaswamy 1989). Condition (i) is an additional condition that ensures Theorem 8.1 holds for the switching periodic lung mechanics model.

10. Numerical simulations of a four-compartment model

In this section, we numerically integrate (19) to illustrate convergence of the trajectories to a stable limit cycle. Here, we assume that the bronchial tree has a regular dichotomy (Section 6). Anatomically the human lung has around 24 generations of airway units. A typical value for lung compliance is $0.1\,\ell/\text{cm H}_2\text{O}$, that is, $\hat{c}_0 = 0.1\,\ell/\text{cm H}_2\text{O}$. (Note that respiratory pressure is measured in terms of centimetres of water pressure.) The airway resistance varies with the branch generation and typical values can be found in Hofman and Meyer (1999). Furthermore, the expiratory resistances will be higher than the inspiratory resistance by a factor of 2 to 3. Here, we assume that the factor is 2.5. Now, based on the values for the 24-generation model and using (50)–(53) we can obtain m-generation models for all $m = 0, \ldots, 23$.

Figures 4 and 5 provide the time responses of the compartmental volumes of a 1-generation and 2-generation lung models, respectively, where we assumed that the applied pressure $p_{in}(t) = 20t + 5$ cm H_2O, $p_{ex}(t) = 0$ cm H_2O, the inspiration time $T_{in} = 1$ s, the expiration time $T_{ex} = 2$ s, and the initial total volume $x_{tot}(0) = 0.25\,\ell$. Figures 4 and 5 clearly show that the states of the 1-generation and 2-generation models converge to limit cycles. Furthermore, after an initial transient behaviour, the steady-state volume in the lung is uniformly distributed over all the compartments, that is, the steady-state value of the volume in each compartment is equal (in both the 1-generation and 2-generation models). Finally, Figure 6 shows the

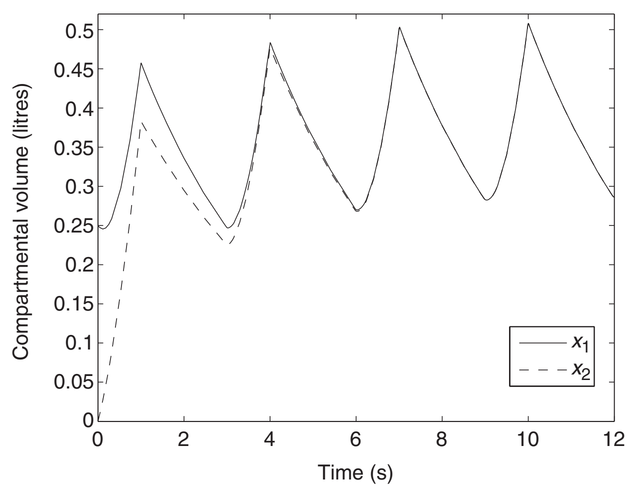

Figure 4. Compartmental volumes vs. time: 1-generation model.

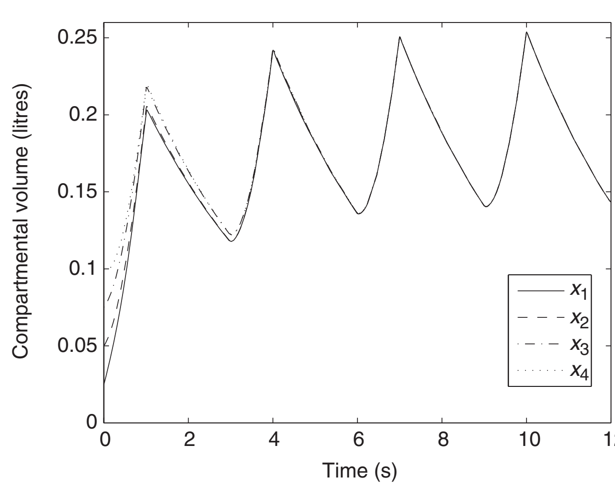

Figure 5. Compartmental volumes vs. time: 2-generation model.

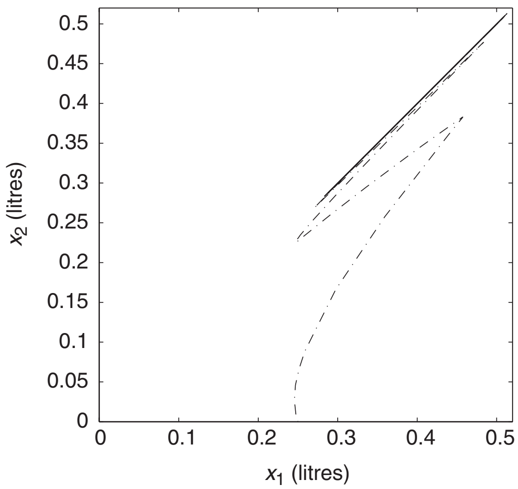

Figure 6. $x_1(t)$ vs. $x_2(t)$: 1-generation model.

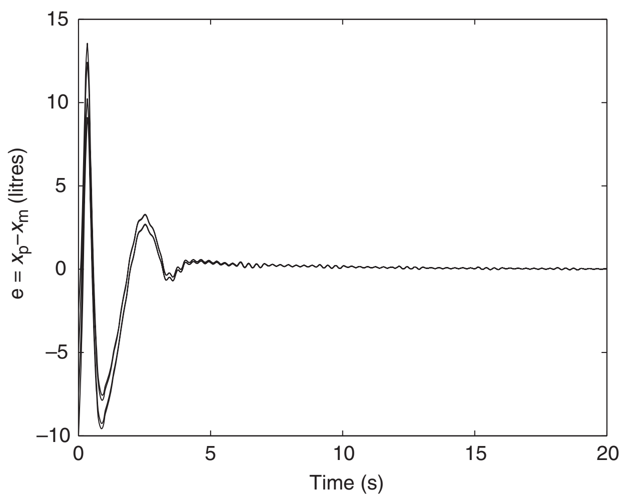

Figure 7. Error vs. time.

phase portrait ($x_1(t)$ vs $x_2(t)$) of the 1-generation model showing the asymptotic convergence of the state to a limit cycle.

Finally, we illustrative the adaptive controller framework of Section 8 on our four-compartment lung mechanics model. The reference model is assumed to correspond to a bronchial tree which has a regular dichotomy architecture (Section 6). Furthermore, we choose a reference model so that all the conditions of Proposition 9.1, and hence, the compatibility conditions of Theorem 8.1 are satisfied. In addition, we let $\Theta_0 = [75, 75, 75, 75]$ and $Q_0 = 5$. Note that no explicit knowledge of the plant model is needed to generate the adaptive control input $u(t)$, $t \geq 0$, given by (66) and the update laws given by (67) and (68). Figure 7 shows the error $x_p(t) - x_m(t)$ vs. time t, verifying that $x_p(t) \to x_m(t)$ as $t \to \infty$. Here, we assumed that the applied pressure for the reference model is $r(t) = \sin(20t) + 5\,\text{cm H}_2\text{O}$ and the inspiration time is $T_{in} = 1$ s and the expiration time is $T_{ex} = 2$ s. Figures 8 and 9 show the controlled phase portrait.

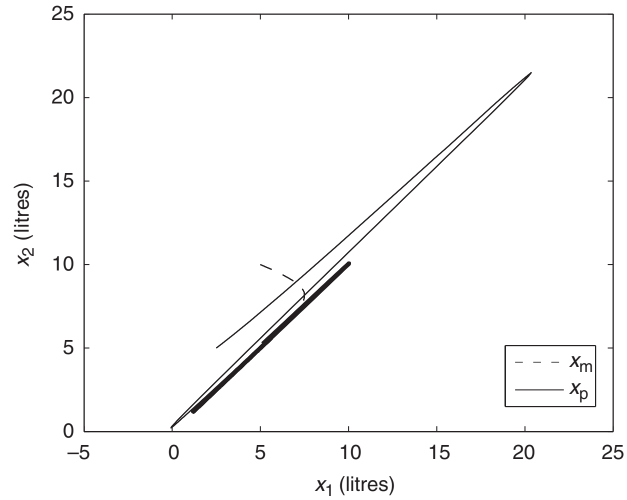

Figure 8. $x_1(t)$ vs. $x_2(t)$: Controlled phase portrait.

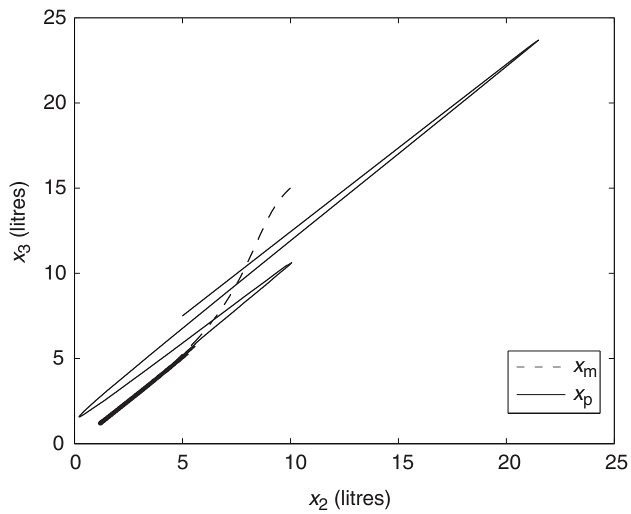

Figure 9. $x_2(t)$ vs. $x_3(t)$: Controlled phase portrait.

11. Conclusion

Respiratory failure, the inadequate exchange of carbon dioxide and oxygen by the lungs, is a common clinical problem in critical care medicine, and patients with respiratory failure frequently require support with mechanical ventilation while the underlying cause is identified and treated. At its simplest, mechanical ventilation is accomplished by the application of cyclically varying positive gas pressure to the trachea. In the absence of patient respiratory effort, it is commonly observed that the lung volumes at end-inspiration and end-expiration rapidly converge to stable steady-state values. However, this does not guarantee that the lungs, viewed as a dynamical system, are stable. Anatomically the lungs are a tree-like structure with repetitive branching into smaller and smaller airways, culminating in the functional units of gas exchange, the alveoli. Stability of end-inspiratory and end-expiratory lung volume does not guarantee that the volumes of individual functional units (the alveoli) are stable.

In this article, we developed a general mathematical model to analyse the behaviour of a multi-compartment respirator and lung mechanics system. In particular, we used compartmental dynamical system theory and Poincaré maps to show that a general multi-compartment dichotomous lung model converges to a stable limit cycle. Furthermore, we extended the analysis to models with a general tree architecture using graph theory. This extension is particularly important since the anatomy of the lungs is significantly more complex than a regular dichotomous model. Finally, we developed an adaptive control framework for the multi-compartmental model of a pressure-limited respirator and lung mechanics system. Specifically, we developed a model reference direct adaptive controller framework where the plant and reference models involve switching and time-varying dynamics. Next, we applied the proposed adaptive feedback controller framework to stabilise a given limit cycle corresponding to a clinically plausible respiratory pattern.

Future work will involve the application of the proposed adaptive control framework for intensive care unit sedation control using appropriate respiratory parameters. Calculation of patient work of breathing requires measurement of a patient-generated pressure/volume loop or work of breathing. Since work of breathing can be measured using a commercially available esophageal balloon (Kallet, Dicker, Katz, and Mackersie 2006), this could serve as a performance variable for intensive care unit sedation. Furthermore, patient–ventilator dyssnchrony may be identified by analysis of pressure/flow wave forms (Nilsestuen and Hargett 2005). Dyssynchrony can be divided into three major categories – trigger dyssynchrony, flow dyssynchrony and cycle (breathing termination) dyssynchrony. While there are a number of components of the pressure/flow wave forms that indicate dyssynchrony, possibly the simplest is the patient respiratory rate (Nilsestuen and Hargett 2005). And it is certainly true that there is a correlation between patient work of breathing and patient-generated respiratory rate. If the goal of sedation is to reduce patient work of breathing, one could target a spontaneous respiratory rate less than some threshold value. This offers the possibility of using respiratory rate as the performance variable for intensive care unit sedation with the proposed adaptive control framework.

Acknowledgements

This research was supported in part by the US Army Medical Research and Material Command under Grant 08108002 and NSF under Grant ECS-0601311.

Note

1. Note that since (3) is a time-varying dynamical system it is typical to denote its solution as $\hat{s}(t, t_0, x_0)$ to indicate the dependence on both the initial time t_0 and the initial state x_0. In this article, we assume that $t_0 = 0$ and define $s(t, x_0) \triangleq \hat{s}(t, 0, x_0)$.

References

Barbini, P. (1982), 'Nonlinear Models of the Mechanics of Breathing Applied to the Use and Design of Ventilators', *Journal of Biomedical Engineering*, 4, 294–304.

Campbell, D., and Brown, J. (1963), 'The Electrical Analog of the Lung', *British Journal of Anaesthesia*, 35, 684–693.

Crooke, P.S., Head, J.D., and Marini, J.J. (1996), 'A General Two-compartment Model for Mechanical Ventilation', *Mathematical and Computer Modeling*, 24, 1–18.

Epstein, M.A., and Epstein, R.A. (1979), 'Airway Flow Patterns During Mechanical Ventilation of Infants: A Mathematical Model', *IEEE Transactions on Biomedical Engineering*, 26, 299–306.

Haddad, W.M., and Chellaboina, V. (2008), *Nonlinear Dynamical Systems and Control: A Lyapunov-based Approach*, Princeton, New Jersey: Princeton University Press.

Haddad, W.M., Chellabonia, V., and Hui, Q. (2010), *Nonnegative and Compartmental Dynamical Systems.*, Princeton, New Jersey: Princeton University Press.

Haddad, W.M., Chellabonia, V., and Nersesov, S.G. (2006), *Impulsive and Hybrid Dynamical Systems*, Princeton, New Jersey: Princeton University Press.

Hofman, W.F., and Meyer, D.C. (1999), 'Respiratory Physiology', in in *Essentials of Human Physiology* (2nd ed.), ed. T.M. Nosek, Florida: Gold Standard Media, Inc. http://www.lib.mcg.edu/edu/eshuphysio/program/section4/4outline.htm

Horsfield, K. (1990), 'Diameters, Generations, and Orders of Branches in the Bronchial Tree', *Journal of Applied Physiology*, 68, 457–461.

Horsfield, K., and Cumming, G. (1975), 'Morphology of the Bronchial Tree in Man', *Journal of Applied Physiology*, 38, 990–1975.

Hotchkiss, J.R., Crooke, P.S., Adams, A.B., and Marini, J.J. (1994), 'Implications of a Biphasic Two-compartment Model of Constant Flow Ventilation for the Clinical Setting', *Journal of Critical Care*, 9, 114–123.

Kallet, R.H., Dicker, R.A., Katz, J.A., and Mackersie, R.C. (2006), 'Effects of Tidal Volume on Work of Breathing During Lung-protective Ventilation in Patients with Acute Lung Injury and Acute Respiratory Distress Syndrome', *Critical Care Medicine*, 34, 8–14.

Kitaoka, H., and Suki, B. (1997), 'Branching Design of the Bronchial Tree Based on a Diameter-flow Relationship', *Journal of Applied Physiology*, 82, 968–976.

Marini, J.J., and Crooke, P.S. (1993), 'A General Mathematical Model for Respiratory Dynamics Relevant to the Clinical Setting', *American Review of Respiratory Disease*, 147, 14–24.

Martinez, S., Michon, G., and Martin, J.S. (1994), 'Inverse of Strictly Ultrametric Matrices are of Stieltjes Type', *SIAM Journal on Matrix Analysis and Applications*, 15, 98–106.

Narendra, K.S., and Annaswamy, A.M. (1989), *Stable Adaptive Systems*, Englewood Cliffs, NJ: Prentice-Hall.

Nilsestuen, J.O., and Hargett, K.D. (2005), 'Using Ventilator Graphics to Identify Patient–ventilator Asynchrony', *Respiratory Care*, 50, 202–234.

Similowski, T., and Bates, J.H. (1991), 'Two-compartment Modeling of Respiratory System Mechanics at Low Frequencies: Gas Redistribution or Tissue Rheology', *European Respiratory Journal*, 4, 353–358.

Thulasiraman, K., and Swamy, M.N.S. (1992), *Graphs: Theory and Algorithms*, New York: Wiley-Interscience.

Wald, A.A., Murphy, T.W., and Mazzia, V.D. (1968), 'A Theoretical Study of Controlled Ventilation', *IEEE Transactions on Biomedical Engineering*, 15, 237–248.

Weibel, E.R. (1963), *Morphometry of the Human Lung*, New York: Academic Publishers.

Wiggins, S. (2003), *Introduction to Applied Nonlinear Dynamical Systems and Chaos* (2nd ed.), New York: Springer.